AN ABSTRACT OF THE THESIS OF

Christopher H.M. Jenkins for the degree of Master of Science in Mechanical Engineering presented on November 16, 1988.
Title: Transient Analysis of a Tennis Racket using PC-based Finite Elements and Experimental Techniques.

Abstract approved: Redacted for Privacy
Clarence A. Calder

Only very recently has modern technology been applied to the design of the tennis racket. In fact, the tennis player of a few hundred years ago would easily recognize today's racket. Although the literature reveals a surprising number of studies on racket mechanics, little work has been reported on the dynamic stresses involved during tennis play. Such investigations lead naturally to questions of fully stressed design optimization.

An AMF/Head "Professional" tennis racket was modeled on an IBMPC-AT using the MSC-PAL finite element code. Experimental verification of the computer model was accomplished in two ways. First, the racket was clamped at the handle, loaded statically, and deflections measured by dial indicator. Next, the racket was instrumented with piezoelectric accelerometers, caused to vibrate in its fundamental mode, and the resulting acceleration-time history recorded on a digital oscilloscope. This data was translated on the IBMPC-AT to reveal the racket's fundamental natural frequency. These experimental results

were then compared to the predictions from the finite element model.

For dynamic loading, the racket was mounted in a test fixture utilizing a spring-loaded arm. Tennis balls were fired from a pitching machine with the acceleration-time history again recorded on a digital oscilloscope. The data was processed on the IBMPC-AT and used as input for the finite element transient analysis, and dynamic stresses in the racket frame were determined. The results are disscused and future research opportunities are indicated.

Transient Analysis of a Tennis Racket Using PC-based Finite Elements and Experimental Techniques

by

Christopher H. M. Jenkins

A THESIS

submitted to

Oregon State University

in partial fulfillment of
the requirements for the
degree of

Master of Science

Completed November 16, 1988

Commencement June 1989

APPROVED:

Redacted for Privacy

Assoc. Prof. of Mechanical Engineering in charge of major

Redacted for Privacy

Head of Department of Mechanical Engineering

Redacted for Privacy

Dean of Graduate School

Date thesis is presented November 16, 1988

Typed by Maureen Jenkins for Chris Jenkins

ACKNOWLEDGEMENT

The author wishes to express his deepest appreciation to his advisor, Dr. Clarence A. Calder. Professor Calder's kindness, encouragement, guidance, and patience provided light when all was dark. Moreover, without the love and support of the author's family - wife Maureen and children Kelli and Amanda - this project would not have been possible. Thank you all.

TABLE OF CONTENTS

LIST OF FIGURES

LIST OF FIGURES (Con't)

LIST OF TABLES

TRANSIENT ANALYSIS OF A TENNIS RACKET USING PC-BASED FINITE ELEMENTS AND EXPERIMENTAL TECHNIQUES

Chapter 1: INTRODUCTION

Tennis most likely dates from the 12th and 13th century France. Modern tennis is usually associated with the period from the late 19th century to present. Until recent time, the tennis racket had changed very little in design or material (wood); in fact, the medievel racket would easily be recognized today (Crowley [1976]).

The first half of the 20th century saw the introduction of laminated wood frames and then the addition of fiberglass overlays. Steel tubing was first used as a frame material in 1967 (Fiott [1978]). Aluminum, fiberglass and other composite materials followed.

Rules governing the design of a tennis racket in play are not stringent and typically specify only the overall geometry and mesh configuration (Fiott [1976]; NAGWS [1986]). Only very recently has modern design technology been applied to the tennis racket, notably computer aided design.

Absence of any published work related to the optimum design of tennis rackets provided motivation for the present study. One of the most basic optimizations that could be applied is the so-called "fully stressed design." According to Gallagher [1973], pg.19:

> "A fully stressed design, abbreviated here as f.s.d., is a design in which each structural member sustains a limiting allowable stress under at least one of the specified loading conditions."

Avrie [1971], pg. 124, gives an algorithm:

> "This condition can usually be achieved by the following technique: given an initial design, compute the stresses in all members in all loading conditions. Increase or decrease each member area in such a way that the largest stress caused by any load condition would just be equal to its limit, assuming that the redesign does not cause a change in member forces. After changing all areas, reanalyze the design and apply the resizing rule again. Stop when no areas require significant change."

It must be noted that, again according to Gallaher [1973], pg. 20: "There is no assurance that an algorithm for the calculation of an f.s.d. will converge to the minimum-weight f.s.d." However, Gallagher [1973] goes on to cite studies showing the differences between fully stressed and minimum-weight designs are small (pg. 30).

Then how does one proceed to find this fully stressed and low-weight design for the tennis racket? The present study is dedicated to that task. In that regard, however, the author must confess that he is not a tennis player and therein may lie a possible source of error.

Chapter 2: SCOPE OF THE RESEARCH PROGRAM

The scope of this research program (RP) was to develop a method to facilitate the fully stressed design optimization of a tennis racket. The method consists of a PC-based finite element model with experimental verification, and transient analysis using experimentally determined dynamic loading data. Results are obtained and discussed.

Objectives of the RP were:

1. survey of the literature;
2. development of a finite element model of a tennis racket;
3. experimental verification of that model;
4. experimental determination of the dynamic loading due to tennis ball impact;
5. and, transient dynamic analysis to determine maximum stress.

The above are symbolically represented in Fig. 2.1.

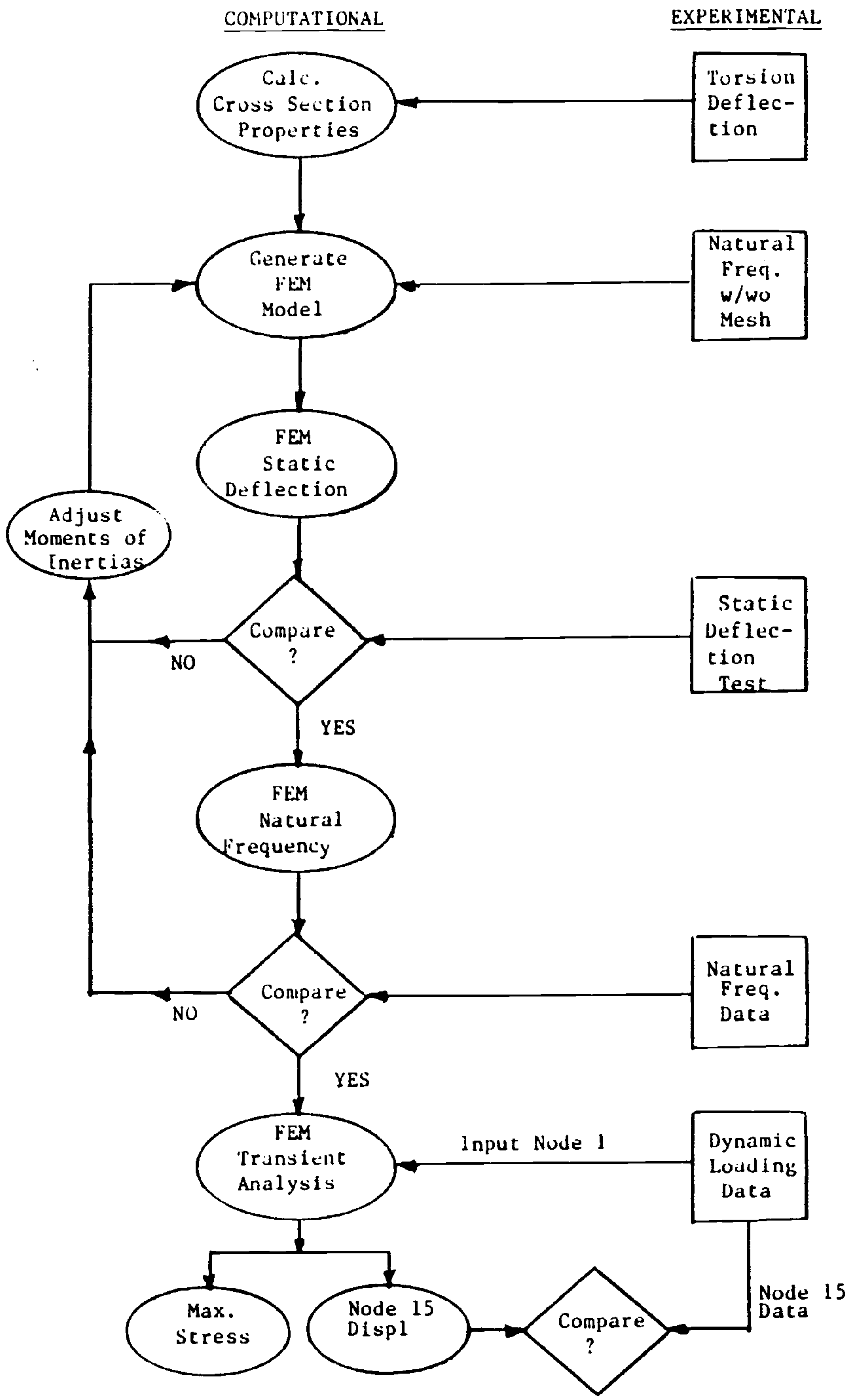

Figure 2.1. Scope of the research project

Chapter 3: THE FINITE ELEMENT MODEL

For testing purposes, an AMF/Head 'Professional' tennis racket was acquired. The frame material is 7005 aluminum [Fiott (1978)] with plastic yoke and string strips (see Appendix 1 for properties of this material).

External dimensions of the racket frame cross section were carefully measured with dial calipers, while frame wall thickness was determined after drilling of a small test hole (see Fig. 3.1).

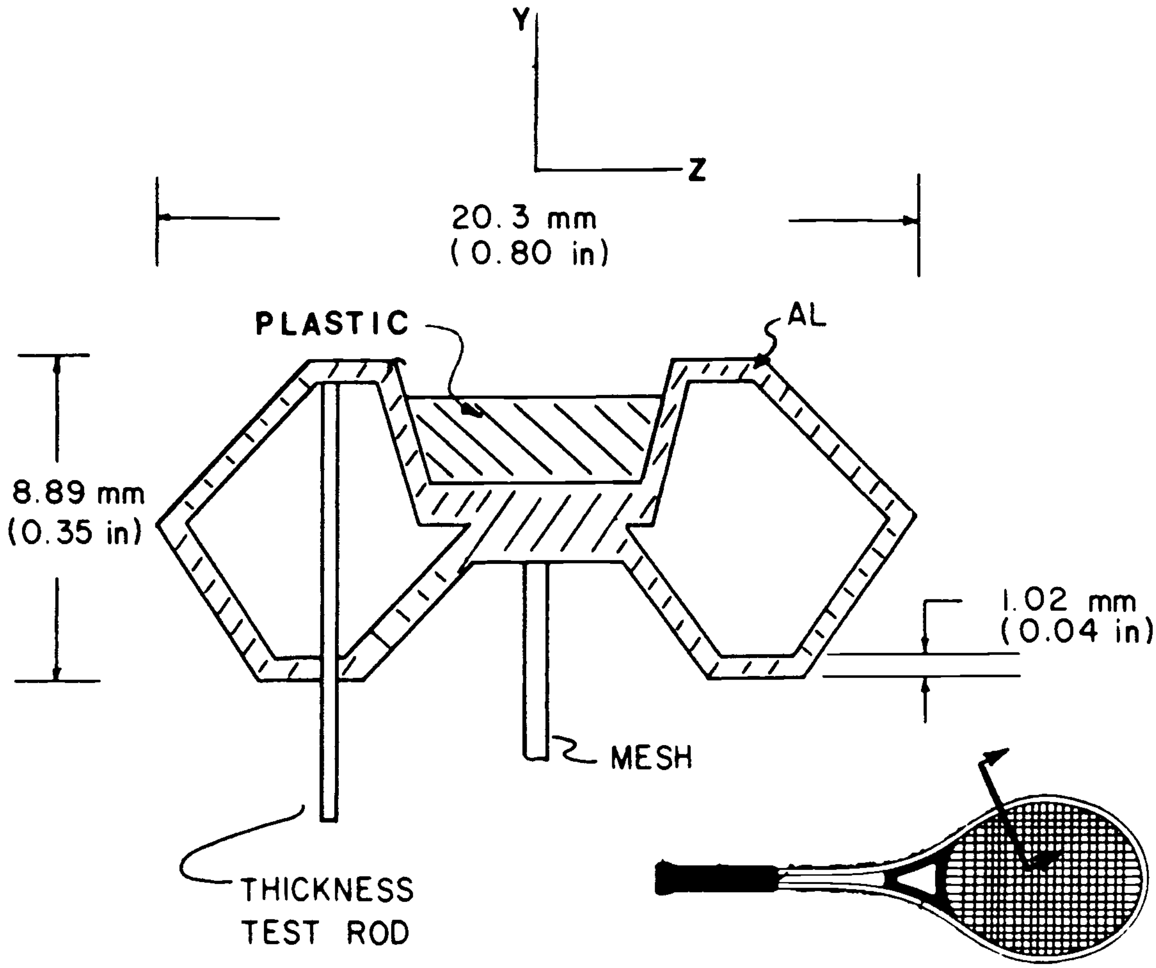

Figure 3.1. Racket frame cross-section

Due to symmetry and constraints on model size, only one-half of the frame, divided about its long axis, was modeled. The overall racket geometry was traced onto a grid sheet; this is, of course, the outside dimension. However, nodes for the FEM beam elements were to exist at the element centroid, i.e., corrsponding to the racket frame controid. From the cross section dimensions, this centroid was computed. Additionally, in the racket head area, nodes were located at each string attachment point, since this is the point of application of racket frame forces and accelerations (from the deformed strings).

To the racket frame tracing, the equation of an ellipse

$$((X-16.8)/5.45)^2 + (Y/4.50)^2 = 1.00 \qquad (3.1)$$

was fit with good results. A computer program was then developed to generate the requisite nodal coordinates from knowledge of string attachment points, centroid location, and the governing elliptical equation.

Along the shaft, a smooth transition was made to longer elements. The terminal node was located along the grip at a position corresponding to placement of the first finger when the racket was comfortably held. Forty-two nodes, numbered and connected sequentially from tip to handle, were thus defined (see Fig. 3.2).

MSC/pal [1984] type 1 beam elements were used. These are primatic elements with six degrees of freedom (d.o.f.) per node (three translation, three rotation), and which include shear and rotary inertia effects (Timoshenko beam).

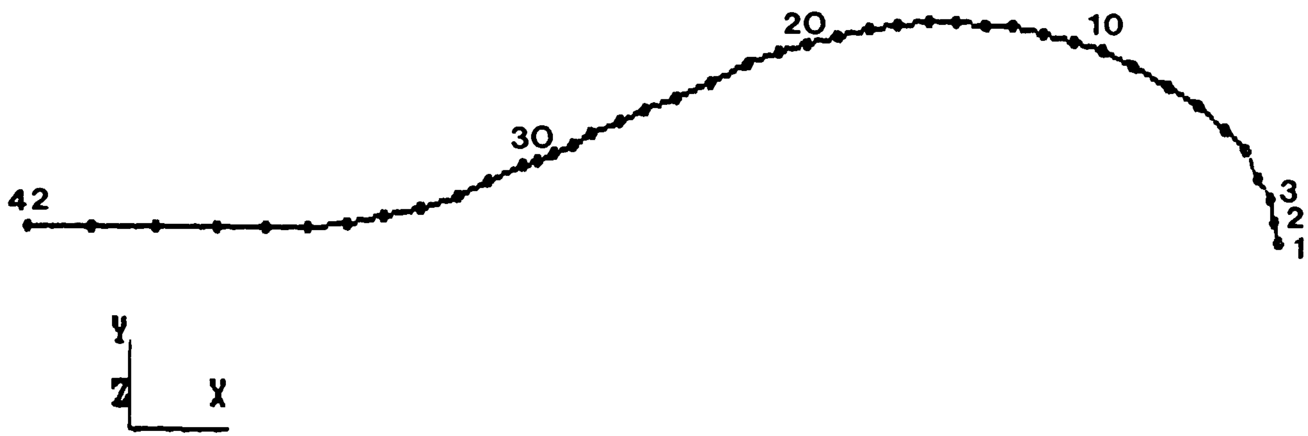

Figure 3.2. Forty-two node finite element model

Shear areas were set equal to zero thus neglecting shear deformation effects. Then at this point, 42 x 6 = 252 d.o.f. were defined. Cross-sectional area, moments of inertia, and torsional moment of inertia must also be defined.

Cross-sectional area was taken to be the effective area of the hollow cross section, i.e., the area defined by the inner and outer perimeters. This has a value of 1.07 cm^2 (0.166in^2).

Moments of inertia were calculated about both axes in the plane of the cross section (see Fig. 3.1) . This was done in the routine tabular method of reducing the section to discrete polygons. The results are:

$$I_{yy}=0.206\ cm^4\ (4.94x10^{-3}\ in^4)$$
$$I_{zz}=0.0367\ cm^4\ (8.81 \times 10^{-4}\ in^4).$$

Determination of the torsional moment of inertia is somewhat more complicated. For solid and built up solid open cross sections, as well as thin-walled open and closed cross sections, analytical methods are readily available. However, care must be exercised in considering this section thin-walled. Following the method outlined in Kollbrunner and Basler [1969], the thin-walled assumption fails (i.e., results in greater than 10% computational error) for:

(i) shear stresses when the ratio of effective area of the cross section to the area enclosed by the wall center line is greater than 0.20;

(ii) torsional moment of inertia when the ratio of effective area of the cross section to the area enclosed by the wall center line is greater than 1.

For the racket cross section, results of the above criteria are as follows:

Effective area (F)= 0.247 cm^2 (0.0382 in^2)

Centerline area (A)= 0.370 cm^2 (0.0574 in^2)

Ratio F/A= 0.666

Clearly, the racket cross section fails criteria (i). As a result, the torsional moment of inertia was determined both analytically and experimentally. Analytically, use was made of Bredt's formula

$$K_c=(4A^2)/[\oint ds/t(s)] \tag{3.2}$$

For constant wall thickness t along a circumference of length l,

$$\oint ds/t(s)=l/t \tag{3.3}$$

This results in a value of K_c=0.0450 cm^4 (1.08 x 10^{-3} in^4).

Experimentally, the racket was clamped to a table, subjected to couples of various magnitudes, and deflection data taken with a dial indicator. Results of this analysis are contained in Table 3.1.

Table 3.1. Determintation of the torsion constant

TRIAL	COUPLE MAGNITUDE T (N·cm)	DEFLECTION (cm)	TWIST ANGLE θ (rad)	TORSION CONSTANT K_e (cm^4)
1	14.09	0.0305	0.00312	0.0613
2	28.19	0.0610	0.00642	0.0613
3	42.30	0.0940	0.00963	0.0596

mean K_e=0.0608

standard deviation=2.3 x 10^{-5}

where $\theta=\tan^{-1}[(\text{DEFLECTION}/3.844)(\pi/180)]$, $K_e=TL/G\theta$

Comparing K_c with K_e , there is a 25% difference. Owing to the very good experimental data (very small standard deviation), the experimental value of the torsion constant was used, K_e=0.0450 cm^4 (0.00146 in^4).

Material properties required in MSC/pal are Young's modulus, shear modulus, mass density, and Poisson's ratio. These are given in Appendix 1.

A suitable choice of boundary conditions was the next phase of model development. At this juncture, however, a comment about problem size limitation is appropriate. MSC/pal has a static problem size limit of 1800 d.o.f. For transient analysis, the problem size limit is 250 d.o.f., but further reduction to 125 d.o.f. (e.g., by use of an eigenvalue-economization method) is required. These methods will not be discussed here and the reader is referred to

Dawe [1983] and Rao [1982] for further details. In this investigation, compliance with the 125 d.o.f. limit was met solely by application of boundary condtions.

Since this investigation was only concerned with in plane bending and no torsion, the following boundary conditions were chosen:

(i) node 42 (terminal or grip node) - all d.o.f. set equal to zero (=6 d.o.f.)

(ii) zero all y-translation d.o.f. (=41 d.o.f.)

(iii) zero all x and z - rotation d.o.f.(=82 d.o.f)

The problem size is now 252-6-41-82=123 d.o.f.

At this point, a discussion of modeling the tennis strings or mesh is in order. First, including the mesh will obviously make compliance with the problem size limitation much more difficult. Second, what significance has the mesh on racket frame dynamics and resultant dynamic frame stresses? To gather some insight into this question, the following experiment was conducted: for a given racket, measure the fundamental natural frequency of vibration with and without a mesh. This experiment is motivated by the knowledge that transient analysis is conducted in MSC/pal by the method of modal superposition (see Chapter 6, Transient Analysis).

So as not to disturb the principal investigative racket frame and mesh, a second racket was used for this test. A Wilson Jack Kramer 'Pro' wood racket was used, first strung, then unstrung with the mesh left attached to keep the racket mass consistent. (For testing procedures, see Chapter 4, Model Verification.) The results are simply this: to within an estimated uncertainty of 0.5 ms, no difference in strung or unstrung natural frequency could be discerned. Hence, the simplifying assumption was made that for a first order analysis, the mesh and its interaction need not be considered. (How this result extends to higher modes of vibration remains to be answered.)

For use in discussing the final transient analysis, the deflection of the mesh under static load was measured. The racket was suspended rigidly in the horizontal plane. A dial indicator was placed below the intersection of strings emanating from nodes 2 and 15 (approximate mesh center). Various loads were applied from directly above the dial indicator. The loads were spread over an area approximately equal to the cross-sectional area of a tennis ball (diameter of about 6.4 cm (2.5 in)). The data is as shown in Table 3.2.

Table 3.2. Determination of mesh spring constant

LOAD (N)	DEFLECTION (mm)	k_m (N/mm)
1.44	0.064	22.7
2.89	0.127	22.8
5.79	0.254	22.8

mean k_m =22.8 N/mm

(130 lb/in)

The MSC/pal finite element program is of the 'batch-process' type. Hence an input data file was generated (Racket.txt) containing the above mentioned model description and is reproduced in Appendix 2.

Chapter 4: MODEL VERIFICATION

Although literature concerning model verification is available (see for example Ebhart [1976], Floyd [1984], Lai [1986], and Steele [1987]), this portion of the finite element analysis is of the utmost importance and often neglected.

In the present study, model accuracy was checked in two ways. Both the static deflection and the fundamental natural frequency of the tennis racket were measured in the laboratory, and these values compared to the finite element predictions. This was an iterative procedure wherein adjustments were made to the model, predictions again checked, adjustments, checks, etc., until the model was acceptably accurate.

A static deflection test was performed by clamping the racket frame to a laboratory table, applying various loads at the racket tip (node 1), and measuring the deflection at the tip with a dial indicator. Results are given in Table 4.1.

From the average value of racket bending stiffness, k_f, the deflection for a 4.45 N (1.0 lb) load is easily found:

$$z=P/k_f \qquad (4.1)$$

$$=4.45\ N/3.45\ N/mm$$

$$=1.29\ mm\ (0.0508\ in).$$

This value is then used to compare with the finite element model given the same static load at node 1.

Table 4.1. Determination of racket frame bending stiffness

LOAD P (N)	DEFLECTION z (mm)	STIFFNESS k_f=P/z (N/mm)
1.41	0.432	3.27
2.83	0.800	3.54
4.24	1.19	3.55
5.65	1.64	3.45

mean k_f=3.5 N/mm

(20 lb/in)

std. deviation= 0.758

To measure the fundamental natural frequency of the racket, a PCB Piezotronics, Inc. model. 303A02 accelerometer was mounted at node 1 of the racket frame (see Chapter 5, Dynamic Loading for mounting details). This is a small accelerometer whose mass (2 gm) should not appreciably affect the frequency measurement. The racket was then placed in a rigidly clamped test fixture (for test fixture details, see Chapter 5, Dynamic Loading). Then the racket was 'plucked' at node 1 (i.e., deformed most nearly into its fundamental mode shape by applying an appropriate bending load at the tip only, then released).

The accelerometer output was recorded (see Fig. 4.1) on a Nicolet digital oscilloscope with floppy disk storage. Simply counting the time between peaks, the fundamental natural period of oscillation is readily shown to be about 32.5 ms with a corresponding natural frequency of 30.8 hz.

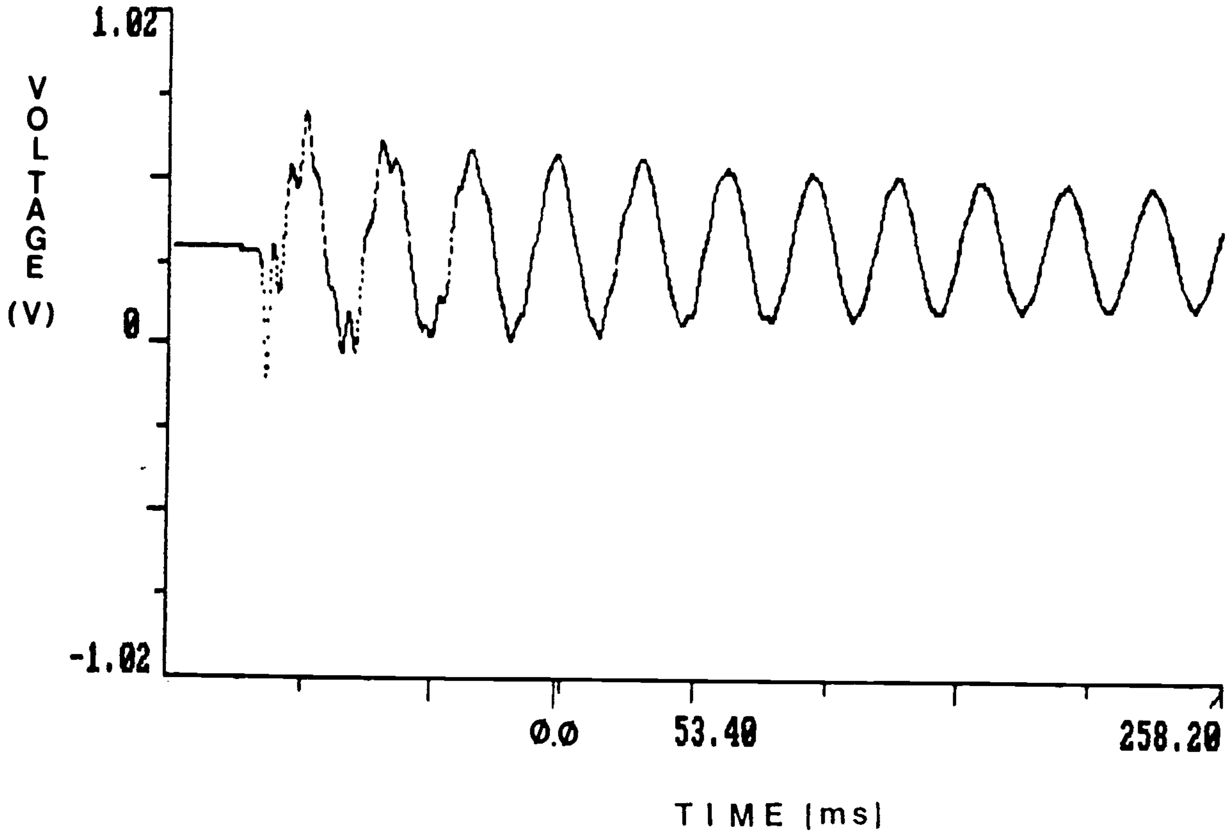

Figure 4.1. Acceleration history of racket at node 1 location giving fundamental natural frequency

The latter value is then used as a check against the finite element predictions.

It was decided that the least precisely known components of the model definition were the moment of inertia values, since these were tediously hand-calculated by a many-step process and the true nature of the cross section interior was never exactly revealed. In as much as torsion phenomena were not to be investigated, only bending moment-of-inertia would be varied in order to bring the model into compliance with experiment. It is next necessary to run both the "stat" and "modes" programs of MSC/pal and compare the results to experiment.

For "stat", a 4.45 N (1.0 lb) load was applied in the z-direction at node 1. "Modes" solves the equations of motion

$$[m]\{\ddot{u}\}+[k]\{u\}=\{0\} \tag{4.2}$$

assuming a steady state, harmonic solution. As "Modes" was invoked, however, it was found unable to run the 123 d.o.f. initially defined model (MSC/pal is purported to run 125 dynamic d.o.f. models); no reason is known for this result. Subsequently, the model was reduced to a 'runable' 111 d.o.f. by changing to a 40 node model through lengthening of the grip-end elements.

The procedure was then to adjust the bending moment of inertia values until the model was accurate to within an arbitrarily chosen small value when comparing static displacement and fundamental natural frequency predictions with experimentally derived values. The iteration was performed keeping these concepts in mind: first, any change in deflection brings about an inverse change in natural frequency, e.g., decrease in moment of inertia (stiffness) results in increased static deflection but decreased natural frequency; second, changes in the moment of inertia about the axis perpendicular to the plane of bending have no effect on static deflection but do effect natural frequency. Unfortunately, due to what is assumed to be numerical instabilities in MSC/pal, the above could never be counted upon. It was a highly non-linear iterative process requiring more luck and art than technique.

Nevertheless, an accurate model was achieved; static deflection was accurate to less than 1% difference while fundamental natural frequency was accurate to less than 2% difference. This required a 17% increase in the moment of inertia value in the plane of bending, and a 90% decrease in the moment of inertia value perpendicular to the plane of bending. The final values for moment of inertia were

$$I_{yy} = 0.241\ \text{cm}^4\ (5.80\text{x}10^{-3})$$

$$I_{zz} = 3.54\text{x}10^{-3}\ \text{cm}^4\ \ (8.50\text{x}10^{-5}\ \text{in}^4\ )$$

The final model definition file is reproduced in Appendix 3 with the associated graphic representation shown in Figure 4.2.

Figure 4.2. Forty-node finite element model

The static deflection results are reprinted in Appendix 10 with the corresponding graphics given in Figure 4.3.

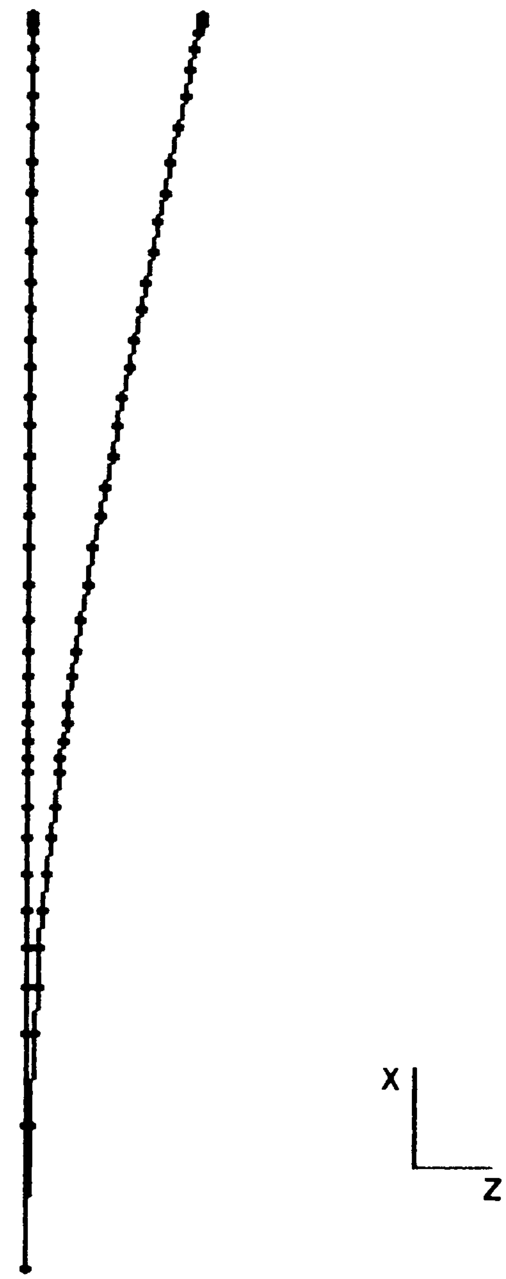

Figure 4.3. Racket frame static deflection under unit load

Listings for the first six modes of vibration are given in Appendix 11, with the corresponding mode shapes reproduced in Figures 4.4 through 4.9. It is noted that MSC/pal performs an accuracy check on the modal values by considering the modal cross-product (orthogonality relation)

$$\{\Phi_i\}^T[m]\{\Phi_j\}=0 \quad , \text{ for } i \neq j$$

where

$\{\Phi_i\}=i^{th}$ mode shape (eigenvector)

$\{\ \}^T$=transpose

$[m]$=mass matrix

MSC/pal lists any modal cross-product with value greater than 0.001 and suggests not using these modes in subsequent calculations (e.g., in transient analysis) due to their questionable accuracy. This was the case for mode no. 2 with modal cross-product value of 0.002713; this mode was not used in transient analysis (see Chapter 6, Transient Analysis).

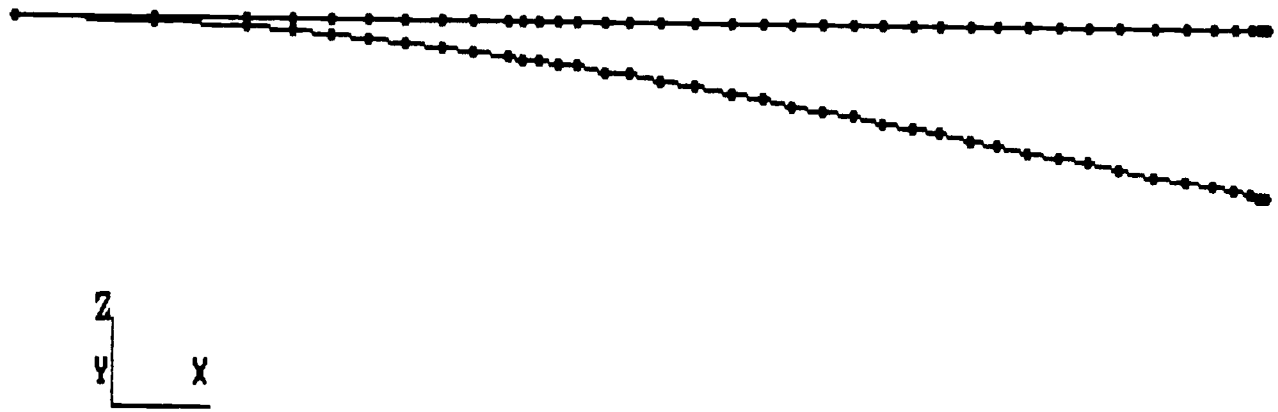

Figure 4.4. Mode no. 1 - 30.4 Hz

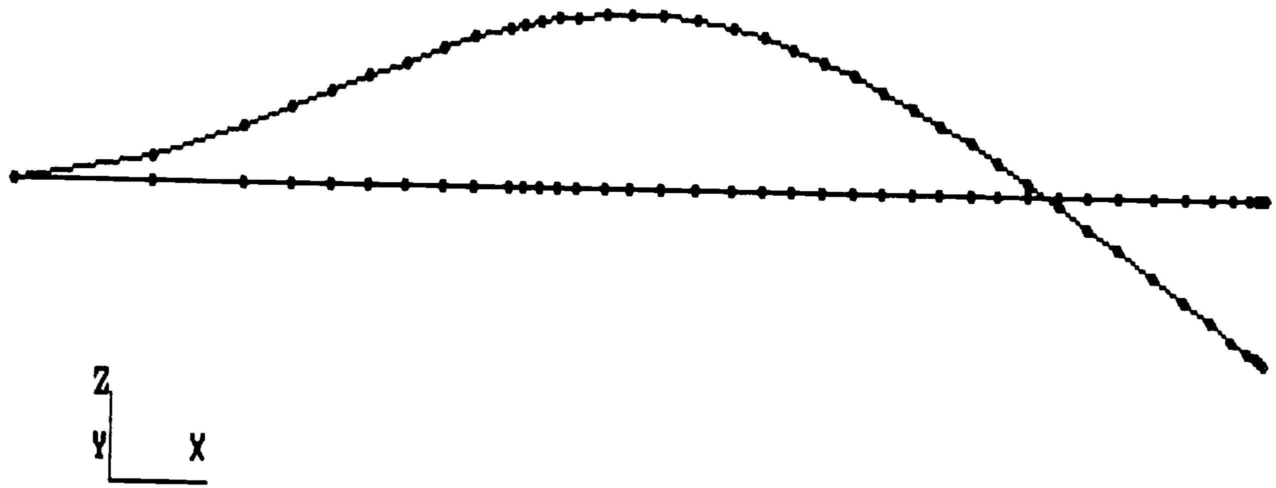

Figure 4.5. Mode no. 2 - 261 Hz

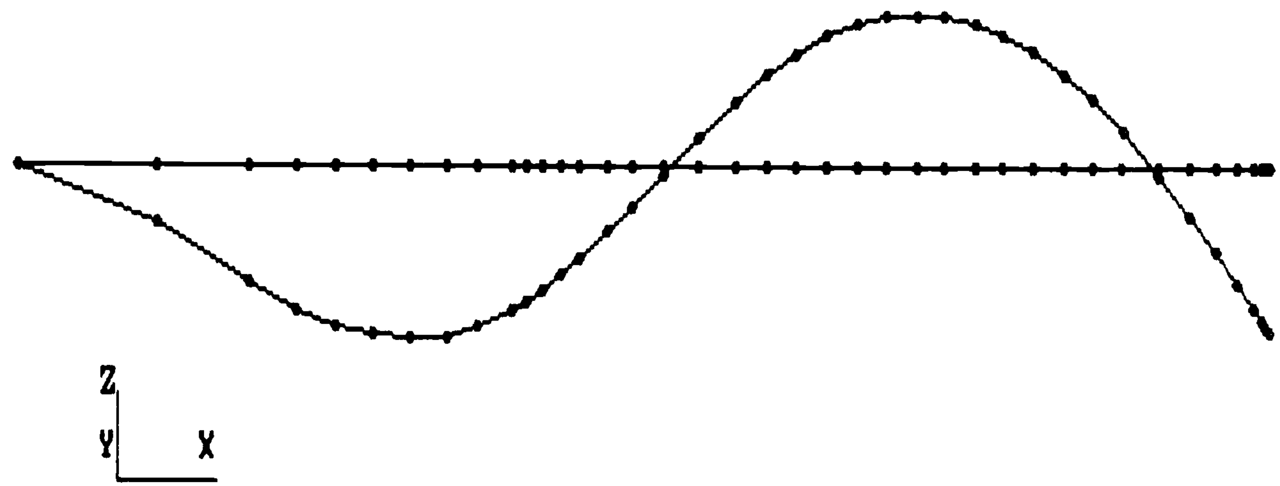

Figure 4.6. Mode no. 3 - 773 Hz

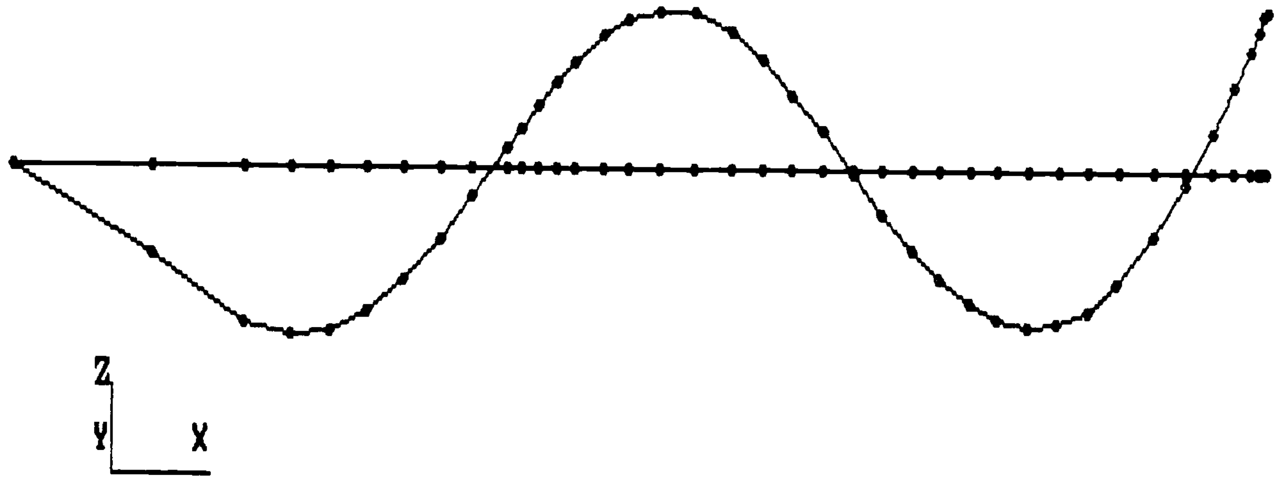

Figure 4.7. Mode no. 4 - 1480 Hz

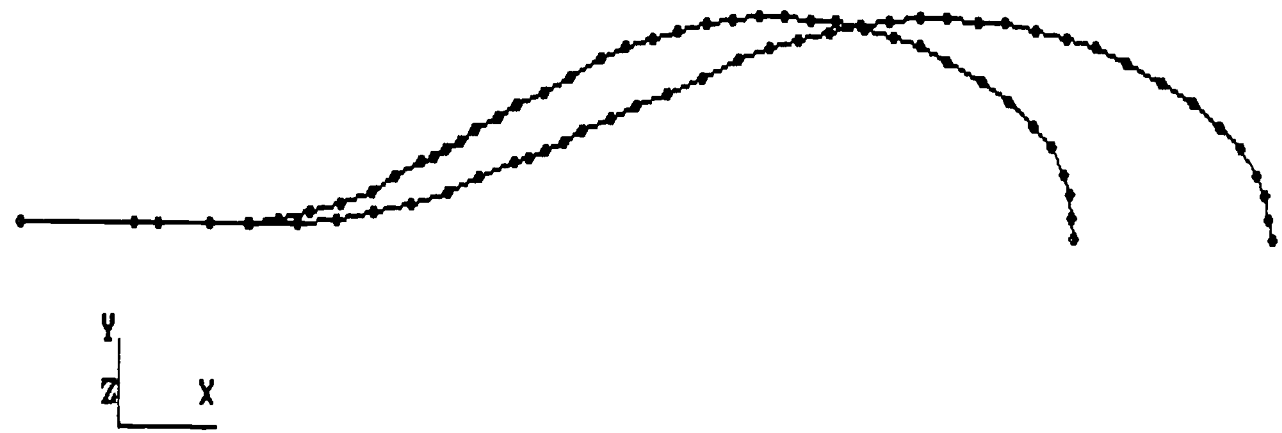

Figure 4.8. Mode no. 5 - 2070 Hz

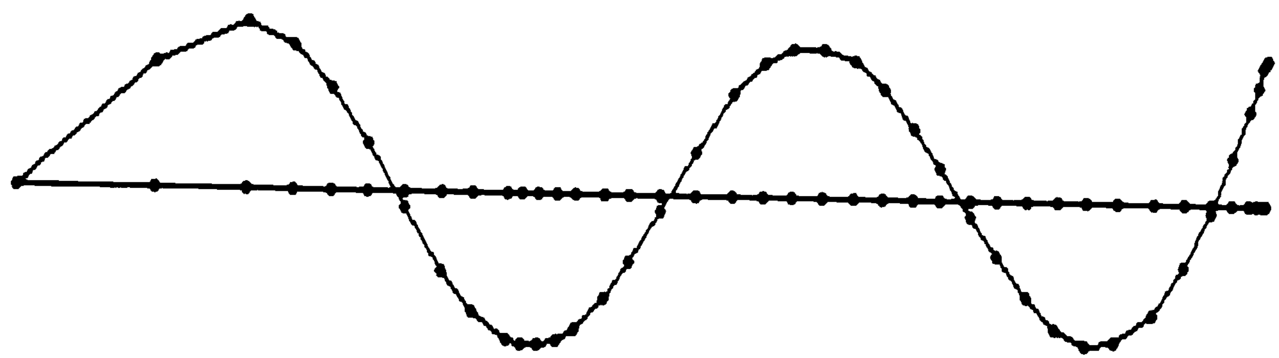

Figure 4.9. Mode no. 6 - 2405 Hz

Chapter 5: DYNAMIC LOADING

What is realistic input for the finite element model? For transient analysis, MSC/pal will accept force, displacement, or acceleration time histories. For the present investigation, it was decided to utilize acceleration time histories taken under conditions that at least somewhat approached those of actual tennis play.

Past researchers have typically used one of three methods for supporting the tennis racket during testing. Baker and Wilson [1978] used a fixed (clamped) end racket. In addition to a fixed end, Baker and Putnam [1974] and Liu [1983] used a free end (racket standing vertically on the grip butt, freely balancing). Elliot et al [1980], Kane et al [1974], and Ohmichi et al [1979] used a live subject to either hold or swing the racket. Hatze [1976] used both fixed and live support. Elliot [1982] used the most sophisticated support, a pneumatically driven holding device.

For purposes of accurate stress analysis, live subjects lead to unrepeatable results, and the fixed or free boundary conditons are unsuitable, producing results either too high or too low, respectively. During actual play, the frame stresses are mitigated by the compliance of the player's arm (but not to the extreme of the free boundary condition). Therefore, in the present study, a compliance support was used as depicted in Fig. 5.1. The spring tension was

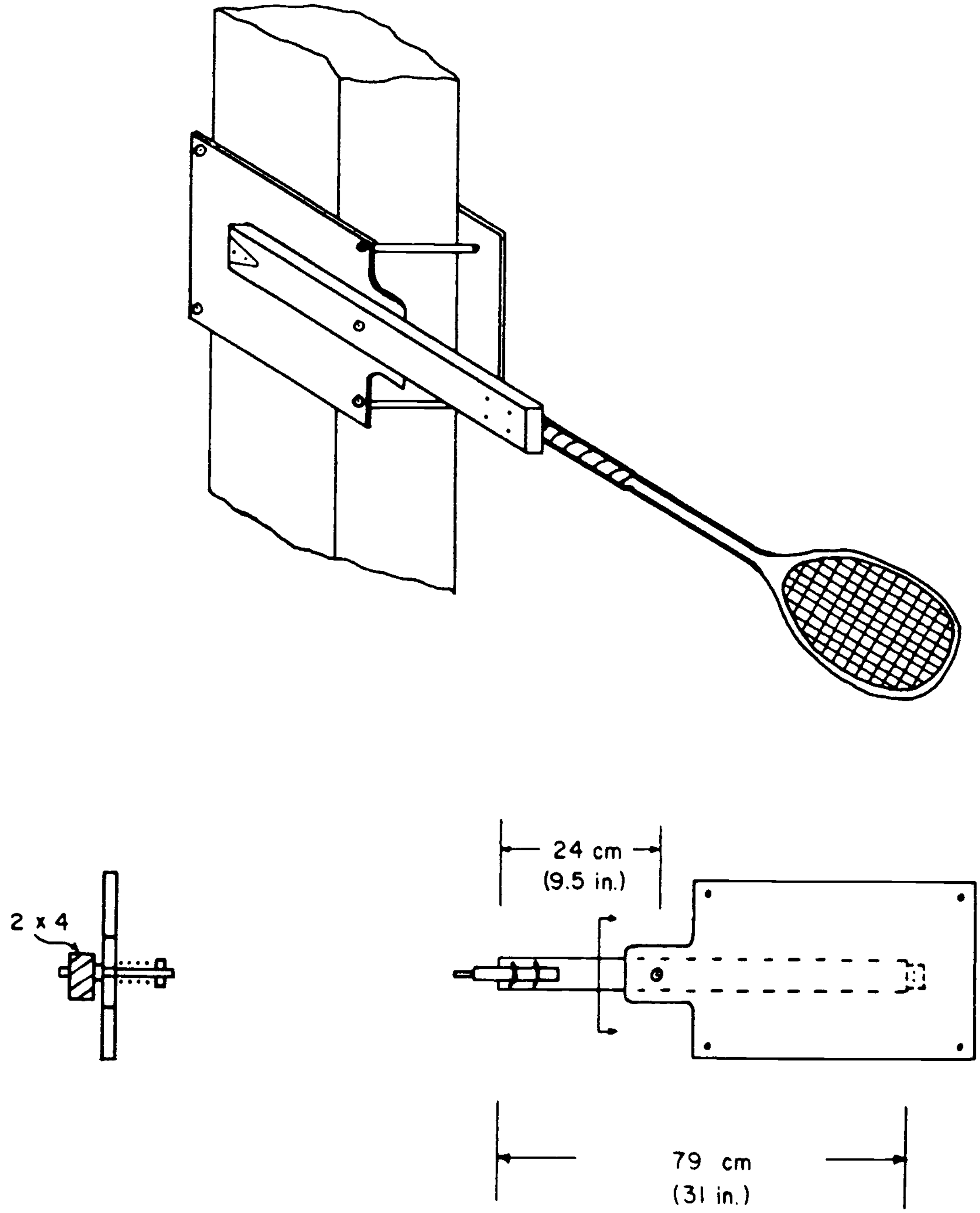

Figure 5.1. Racket holding fixture

adjusted to give the same deflection under dynamic loading as that of a person firmly holding the racket (but not swinging). The spring used had a stiffness given by k_h=6.5 N/mm (37 lb/in).

Once the racket was secured to the holding fixture, the dynamic loading was provided by an electro-mechanical pitching machine (which 'squeezes' out a ball through rapidly spinning rubber wheels). The machine was placed approximately 6 m (20 ft) from the racket. Ball velocity at the racket was expected to be (from earlier work done by Fruend [1986]) between 27 m/s (87 ft/s) and 23 m/s (75 ft/s). These speeds are similar to those reported in the literature (see, for example, Ebert [1976] and Plagenhoef [1982], and were reasonable for the present study). Ball weight was 0.579N (0.130 lb).

PCB Model 303A02 accelerometers were positioned at several locations about the racket frame. (See Appendix 4 for accelerometer data.) Since the accelerometers mount with threaded studs, small threaded plexiglass mounting blocks were epoxied to the frame. (It was assumed that, due to the lightness of both the accelerometer and blocks, the frequency response of the racket was not changed significantly.) Locations of accelermoters were at nodes 1, 8, 15 and 23. Output from the accelerometers was then routed to a power supply and then to a Nicolet digital oscilloscope for subsequent storage on floppy disk.

Since in the present study only pure bending was of interest, only data associated with central hits was desired (as opposed to off-center hits). In order to verify the location of ball impact, a piece of carbon paper was taped to the mesh prior to each loading. This gave a reasonable estimate of the center of impact and allowed only pertinent data to be saved. The mesh was wiped clean with alcohol prior to each new loading.

Figures 5.2 and 5.3 show acceleration time histories for node 1 for a central hit. The impact center associated with this loading is located by imagining lines drawn perpendicular to one another and passing through nodes 2 and 15 (see Fig. 4.2, Chap. 4, Model Verification). Data in Fig. 5.2 was taken at 20 μs/digital point, while in Fig. 5.3 at 10 μs/pt. Figure 5.3 data was used in the transient analysis which follows (Chap. 6, Transient Analysis).

It is interesting to note a correlation of this data with the reported literature. Brody [1979] found dwell times (the duration of time that the ball is in contact with the strings) on the order of 5 ms. Reference to Figs. 5.4 and 5.5 (corresponding respectively to Figs. 5.2 and 5.3 above) shows the principal acceleration peak to be on the order of 4 ms. This correlates well with the above-mentioned finding.

Figure 5.6 shows the acceleration history of node 15 for the same loading event as above. Use will be made of this in Chap. 7.

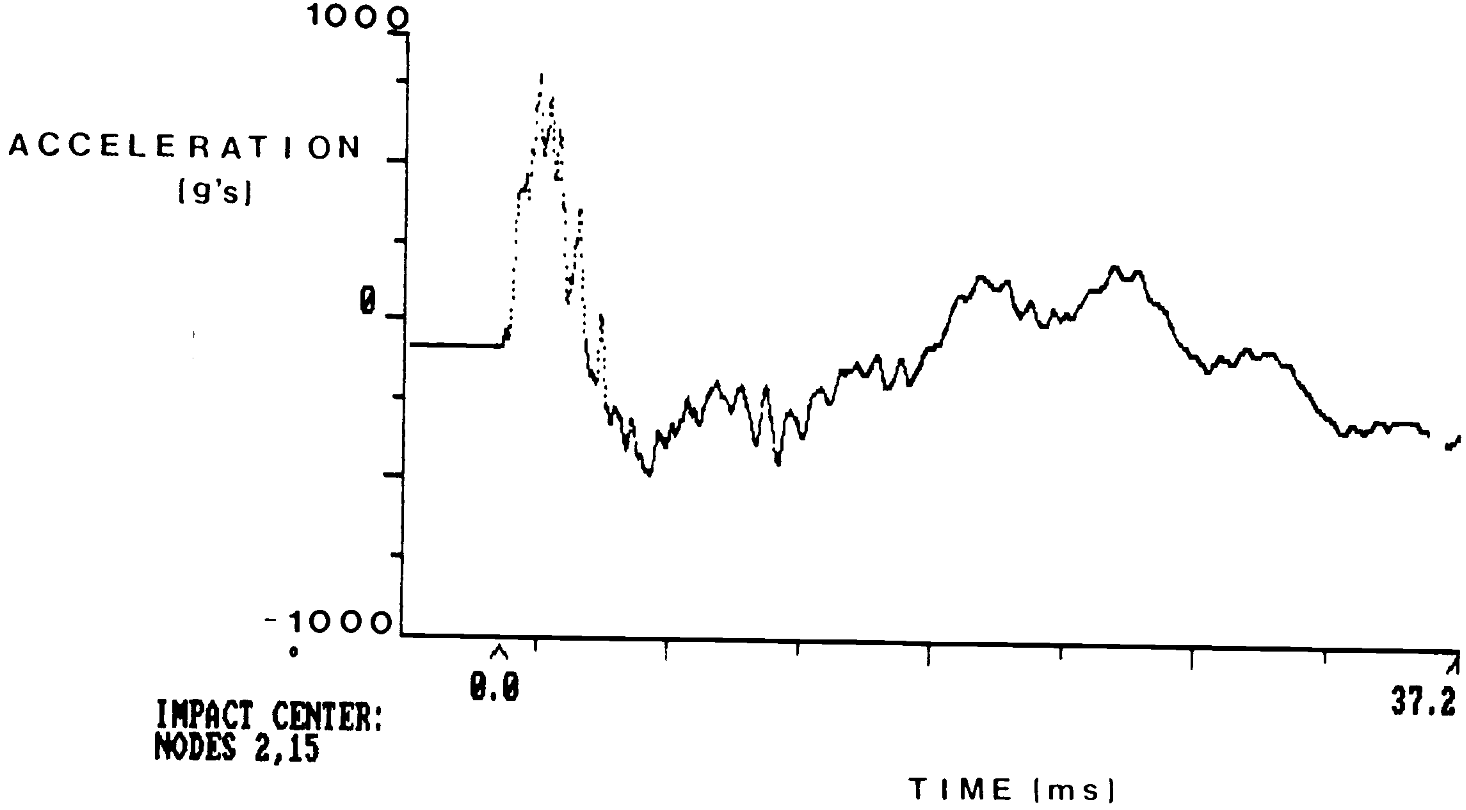

Figure 5.2. Acceleration for node 1 for central impact during dynamic loading (20 μs/pt)

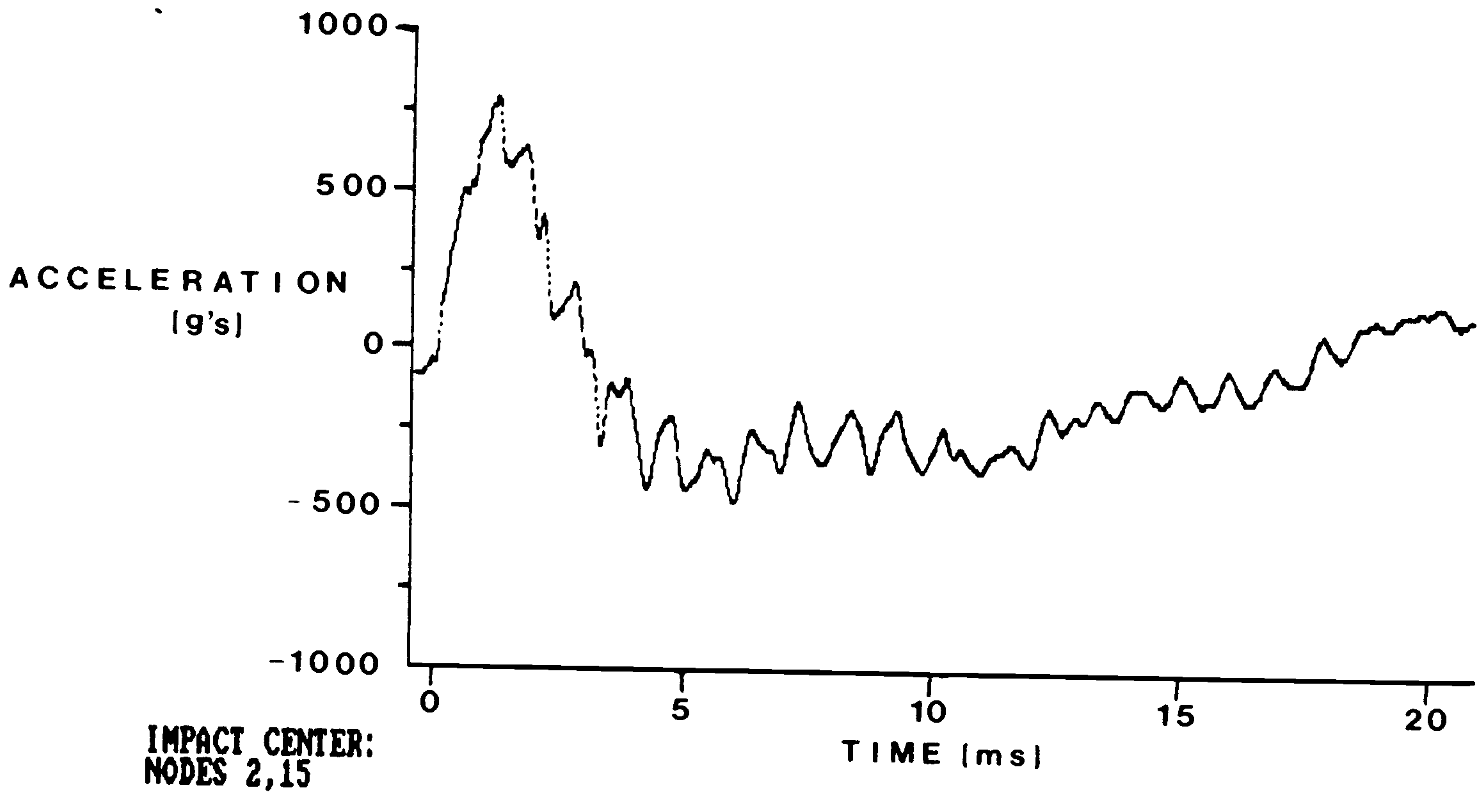

Figure 5.3. Acceleration for node 1 for central impact during dynamic loading (10 μs/pt)

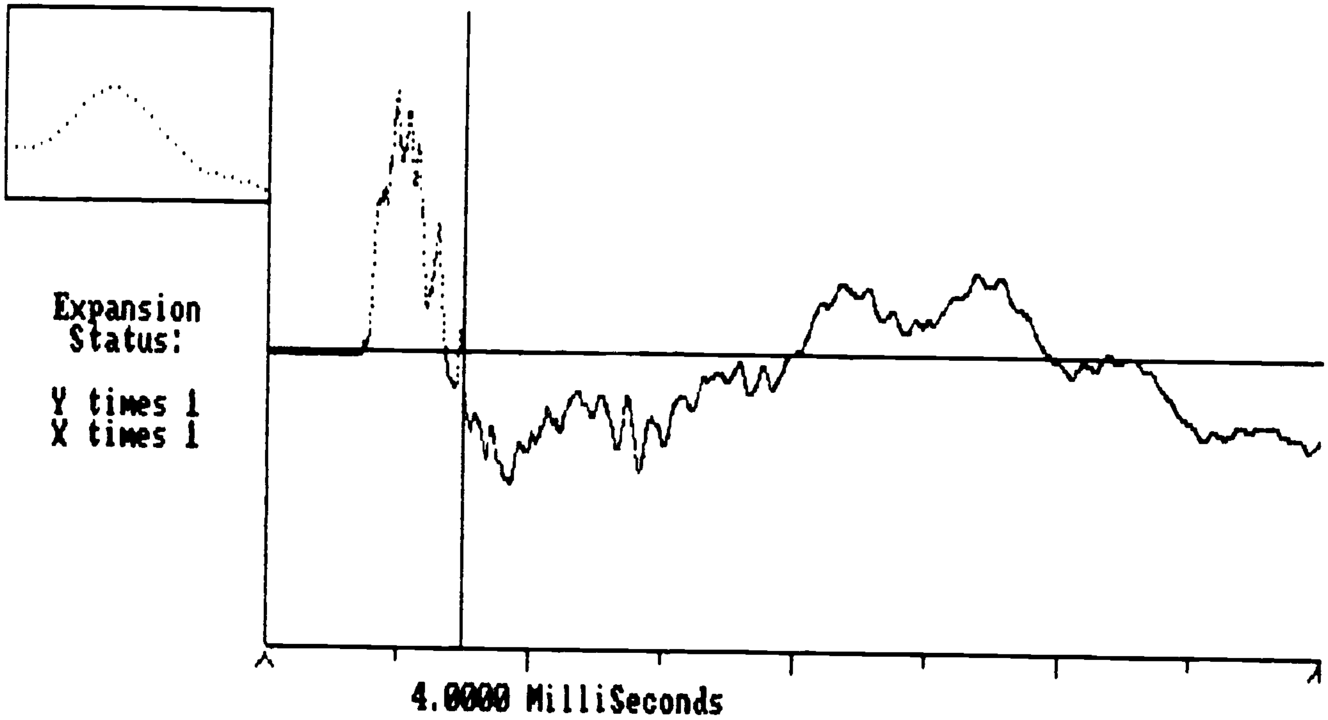

Figure 5.4. Principal acceleration peak time (20 μs/pt)

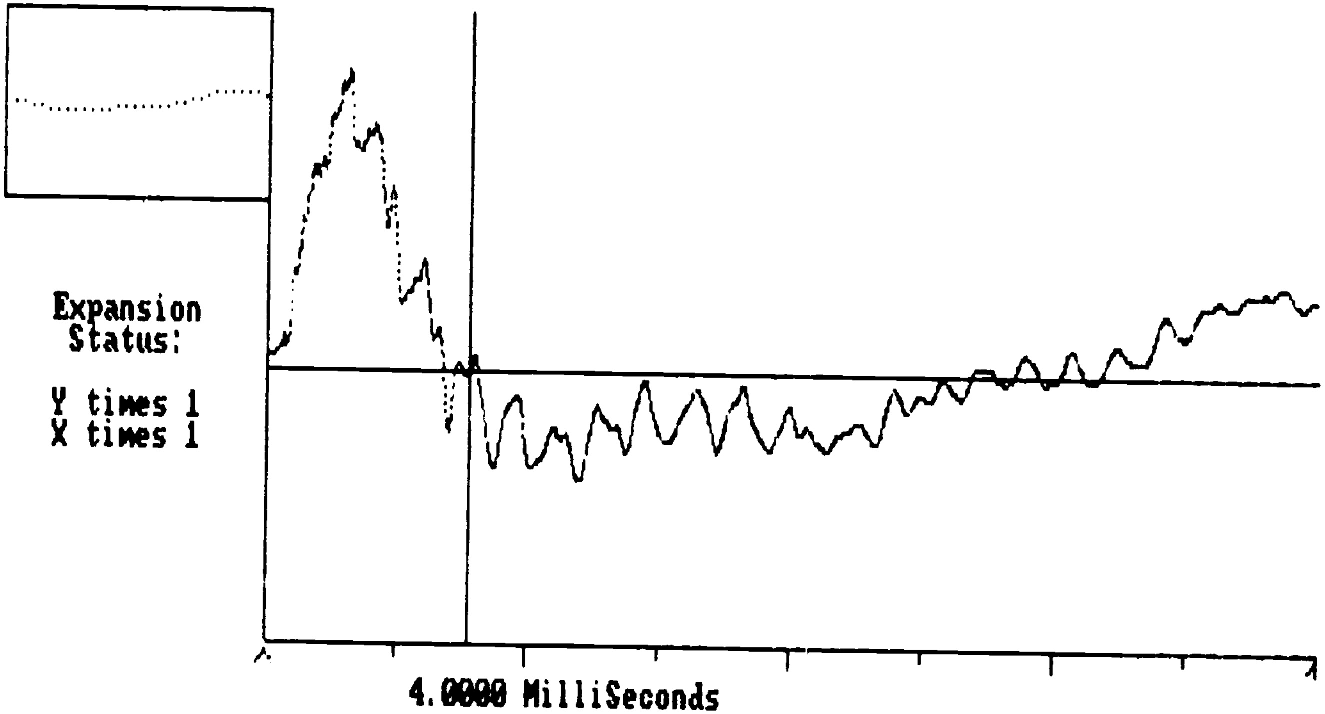

Figure 5.5. Principal acceleration peak time (10 μs/pt)

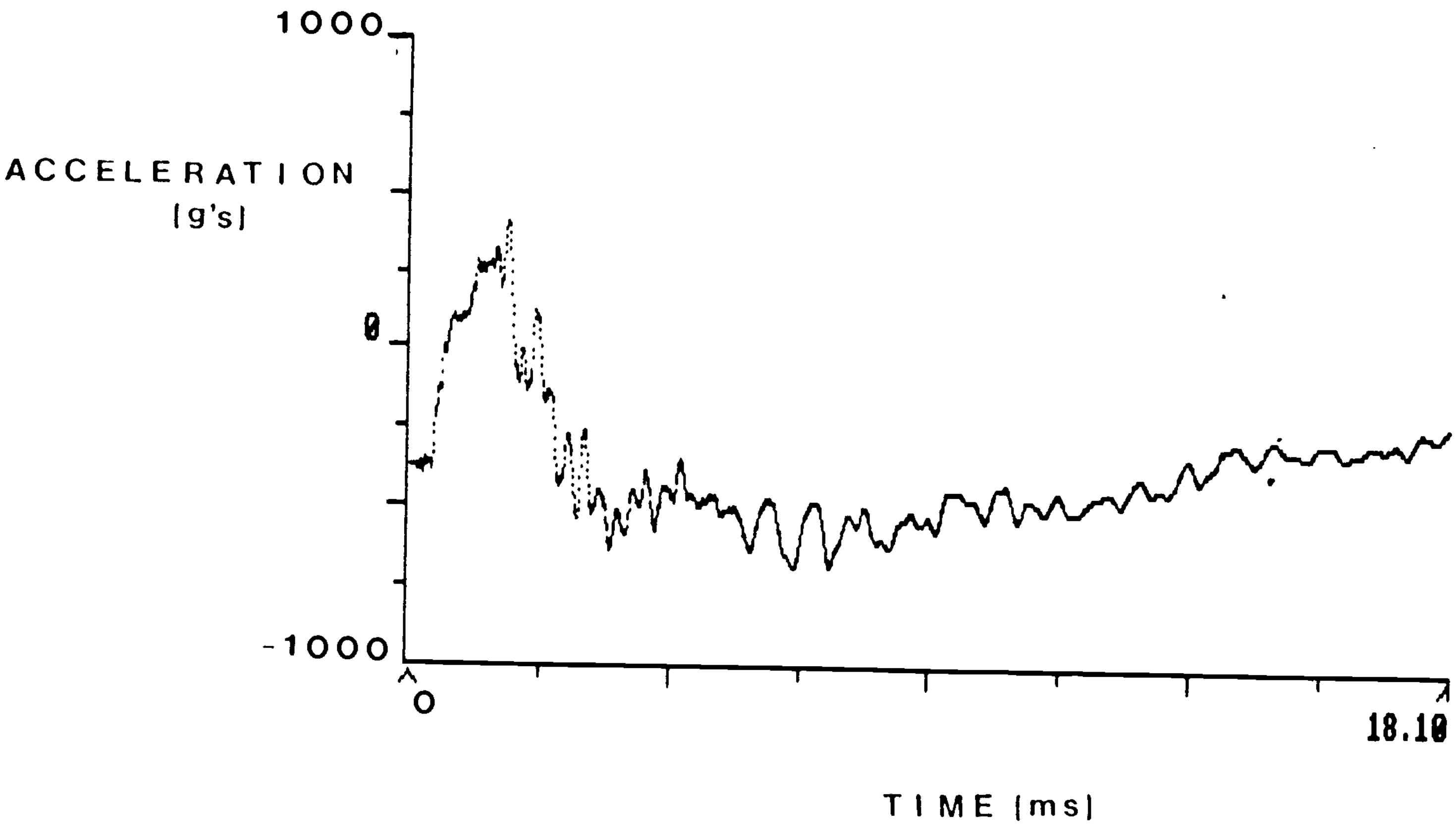

Figure 5.6. Acceleration history for node 15 for central impact during dynamic loading

Chapter 6: TRANSIENT ANALYSIS

In performing transient analysis (i.e., solution of a time-dependent response to a time-varying stimulus) in MSC/pal, a command file is used (see Appendix 5) with the following parameters specifed:

- damping
- excitation type
- excitation definition
- mode shapes

Each of these is now considered in turn.

Damping is specified as a percent of critial damping (ζ) for each mode. In order to estimate this value for the tennis racket, use was made of the logarithmic decrement (e.g., see Thomson [1981], pg. 30):

$$\delta=(1/n)[\ln(X_o/X_n)] \qquad (6.1)$$

where

X_o= any reference peak amplitude, and

X_n= any peak amplitude n cycles later.

Now, for small damping ratio ζ , it can be shown that

$$\delta \approx 2\pi\zeta \qquad (6.2)$$

from which ζ is readily found. Now refer to Figure 6.1 (see Fig. 4.1, Chap. 4 for the description) and the associated Table 6.1 of voltage values (see Apps. 6 and 7 for a complete listing of voltage values and a listing of program 'readit' used to obtain these values while working within the 290-Advance software [1987]).

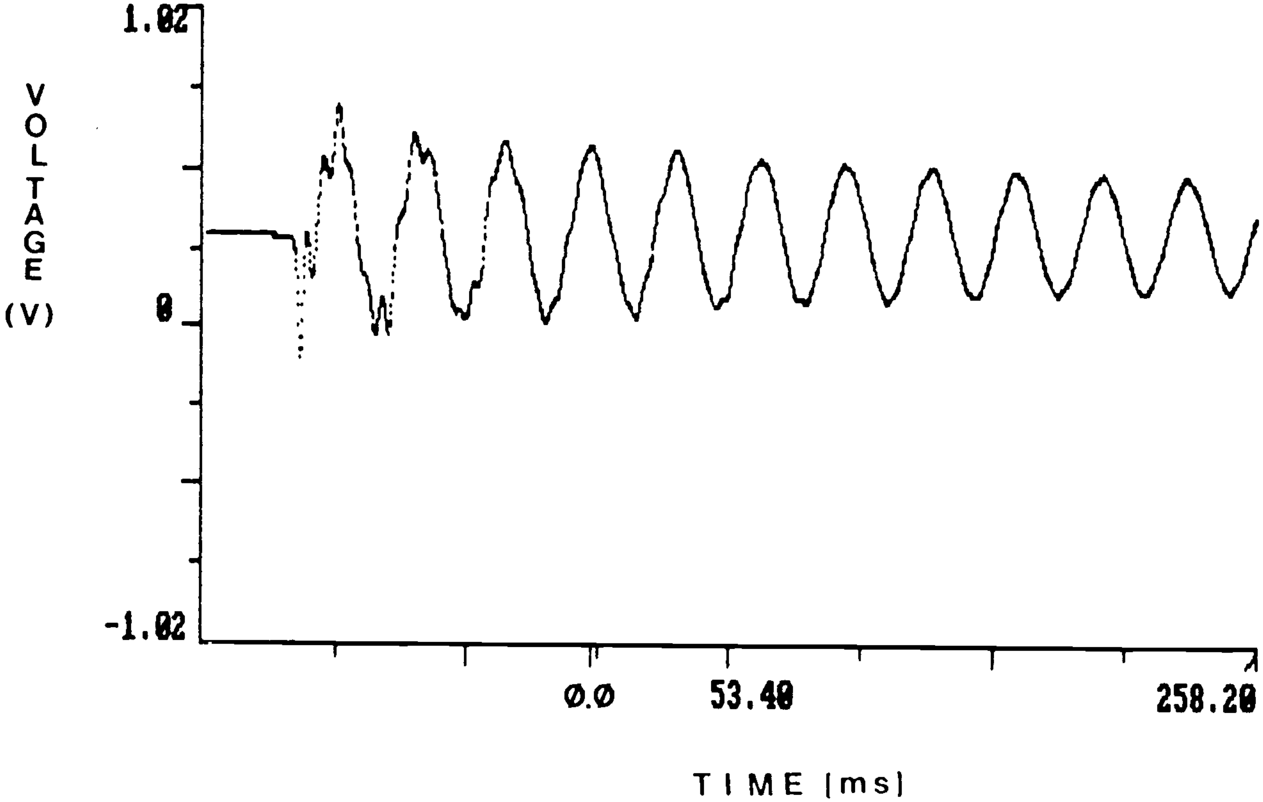

Figure 6.1. Acceleration history of racket at node 1 location giving fundamental natural frequency

Table 6.1. Voltage values for damping determination

X_i	Time (ms)	Voltage (V)
X_0	0.0	0.5795
X_1	32.8	0.5725
X_2	66.4	0.5410
X_3	99.2	0.5265
X_4	132.8	0.5245
X_5	164.8	0.5095
X_6	199.2	0.4995
X_7	230.4	0.4895

The value of ζ can be found as

$$\zeta \approx (1/2\pi)[(1/7)\ln(X_0/X_7)]$$
$$=(1/2\pi)[(1/7)\ln(0.5795-0.31)/(0.4895-0.31)]$$
$$=0.0092$$

The dc-offset is 0.31 V and we in effect average over a number of cycles. Since the racket damping is less than 1% of critical damping, and since the damping is unknown in the higher modes but assumed less than 1% also, the damping parameter was set to zero in the present work.

MSC/PAL allows for either displacement, force, or acceleration time-histories as transient input. It was hoped that acceleration time-histories from dynamic loading (see Chap. 5, Dynamic Loading) would be used directly as input. Unfortunately, no results were ever obtainable in MSC/PAL using this loading, and no reason is known for this occurance. It was then decided to use displacement time-histories as input.

In order to obtain displacement time-histories for input, use was made of the fact that displacement is the second time integral of acceleration, that is

$$z=\int\left(\int \ddot{z}\ dt\right)dt+v_0 t+z_0 \qquad (6.3)$$

where

z = displacement

$\ddot{z}$ = acceleration

v_0 = initial velocity

z_0 = initial position

In the present work, both z_0 and v_0 may be taken as equal to zero.

Use was also made of a numerical integration routine in the 290-Advance software [1987]. The results of those integrations are shown in Figs. 6.2 and 6.3. The integrations are taken over the full time record of the dynamic loading (Fig. 5.3, Chap. 5) which helps to qualitatively verify the reliability of such integrations. However, in that the ball dwell time was established at approximately 4 ms (see Chap. 5, Dynamic Loading), the acceleration record was again integrated, now from zero to approximately 4 ms. This more accurately represents the actual loading and results are shown in Figs. 6.4 and 6.5.

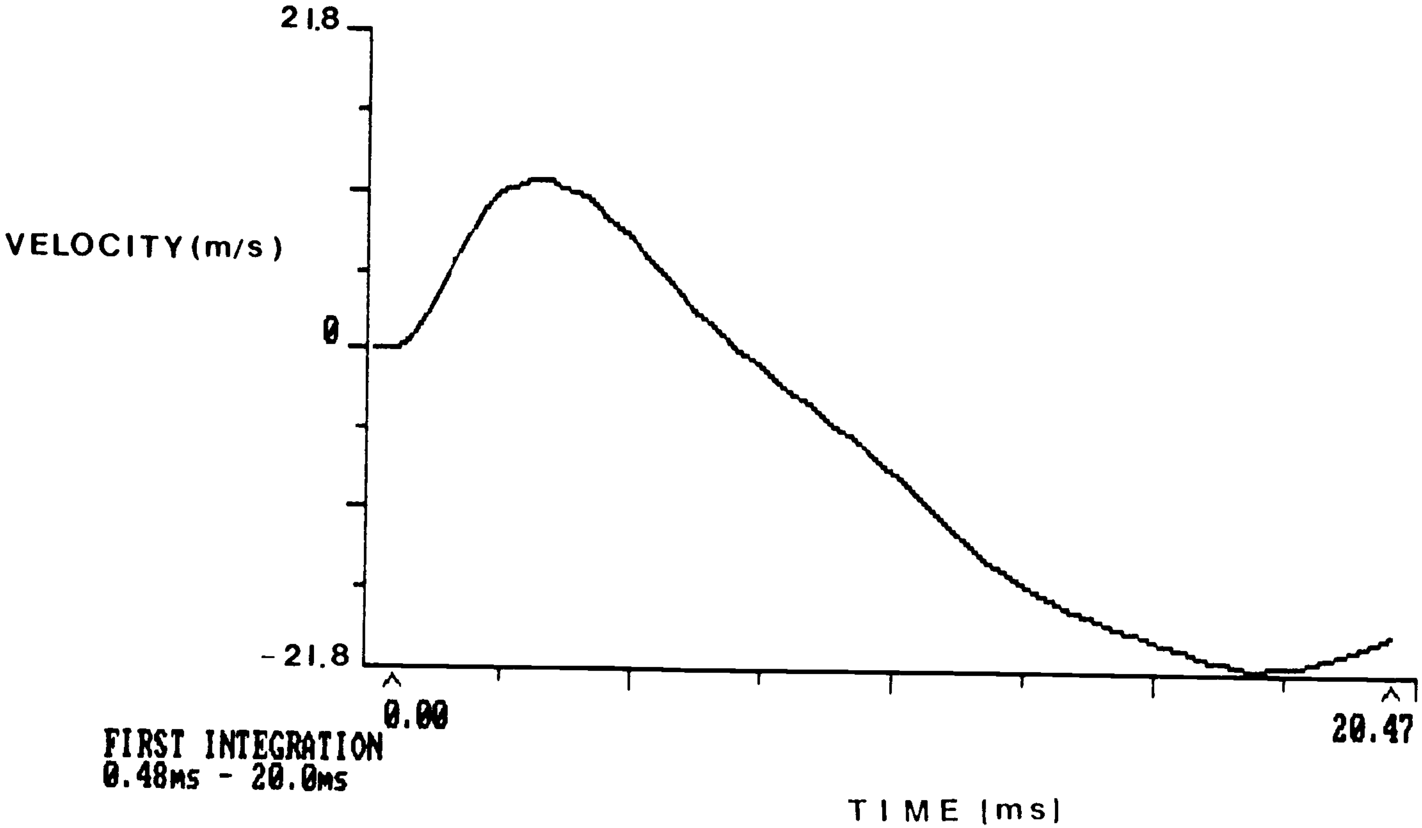

Figure 6.2. Velocity history for node 1 for central impact during dynamic loading (full record)

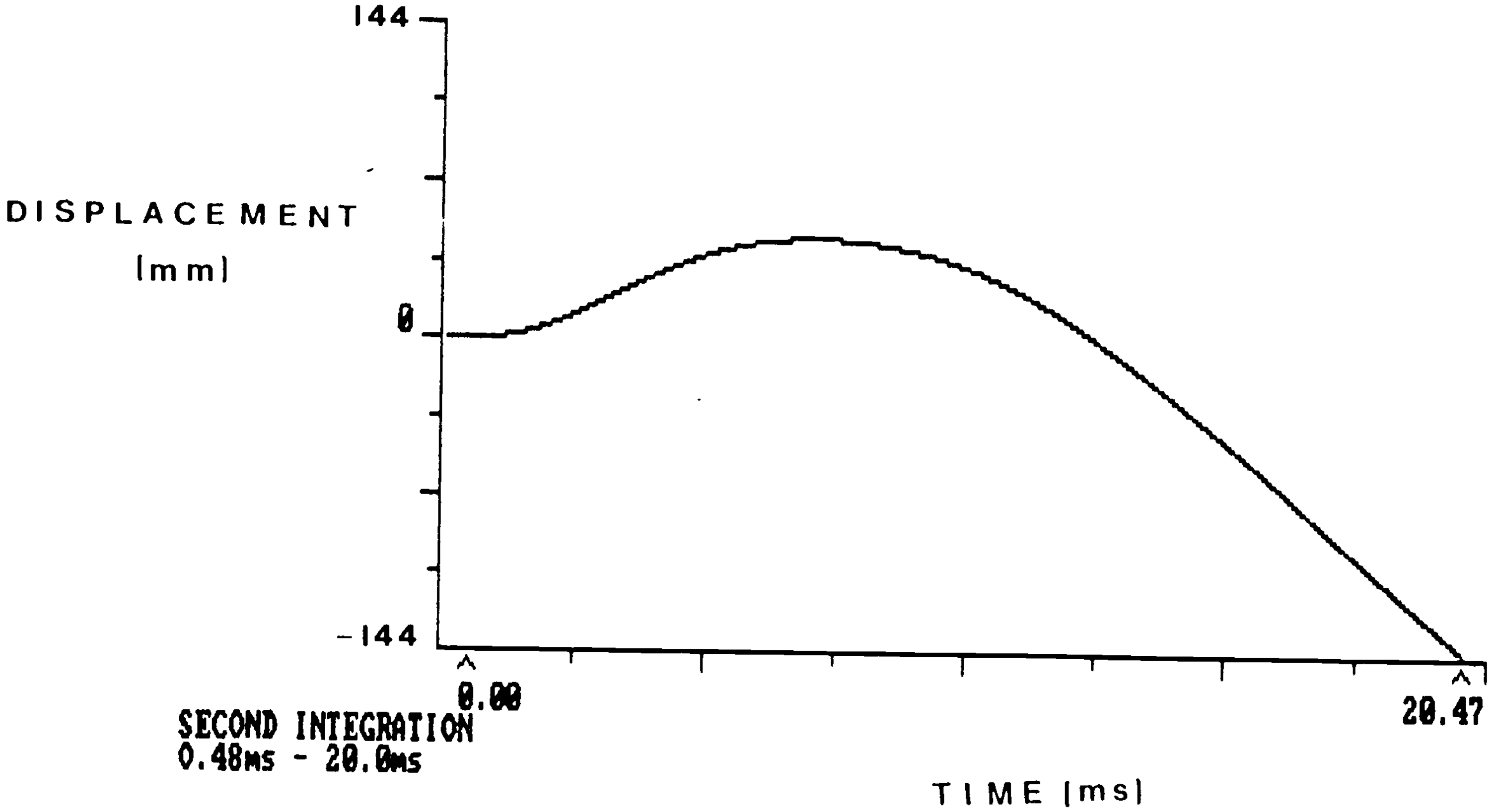

Figure 6.3. Displacement history for node 1 for central impact during dynamic loading (full record)

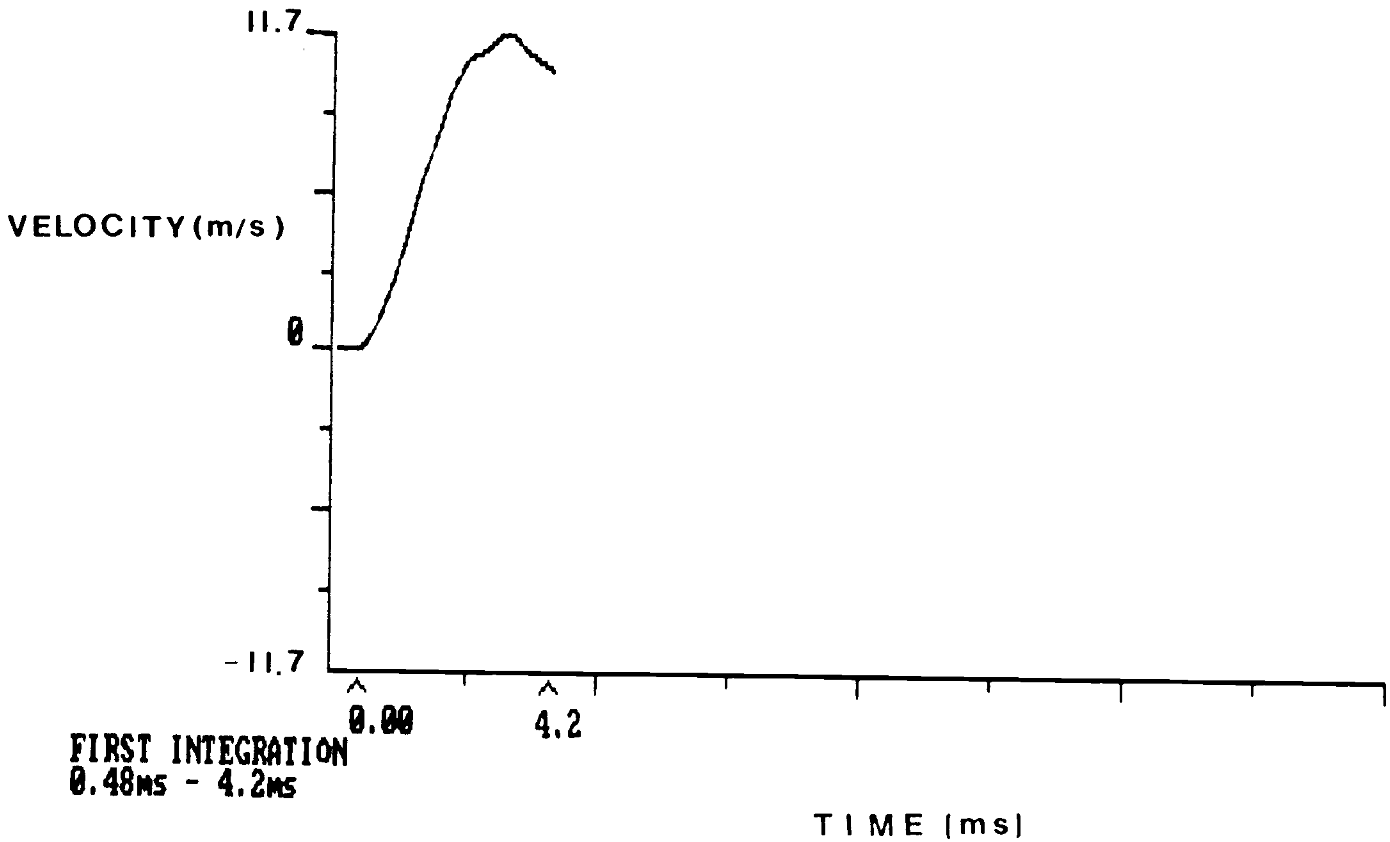

Figure 6.4. Velocity history for node 1 for central impact during dynamic loading (partial record)

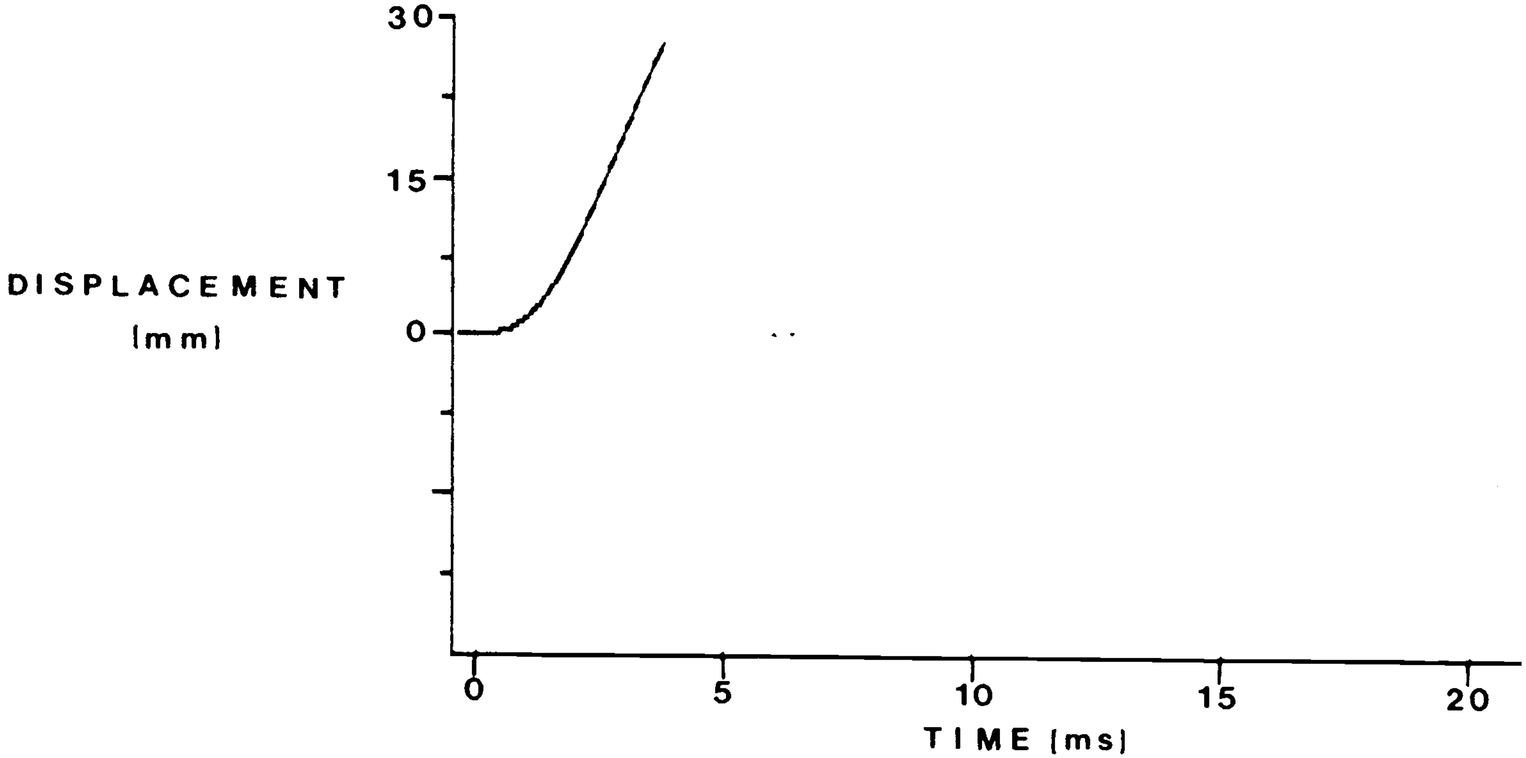

Figure 6.5. Displacement history for node 1 for central impact during dynamic loading (partial record)

Thus Fig. 6.5 represents a 'displacement loading' time-history corresponding to the acceleration loading time-history. Discrete value of Fig. 6.5 (necessary for the command file) were generated in the 290-Advance software [1987] using program 'readit.' These are reproduced in Appendix 8. One can make a quick order-of-magnitude check on the displacement loading record : maximum displacement is seen to be about 27 mm (1.1 in) which is certainly reasonable.

The excitation definition consists of setting a number of parameters along with the discrete listing of the loading (displacement) time-history. In what follows, it was assumed that the results of interest (e.g., maximum stress) would occur during the loading portion of the rackets transient response. Hence the total time for analysis was set at 4.2 ms. The time step, T_i , for numerical integration was set at 0.2 ms. This is consistent with the common rule of thumb that the time increment be less than or equal to 1/10 the fundamental period (see, e.g., Clough and Penzien [1975], pg. 108). In the present case then,

$$\begin{aligned} T_i &\leqq 33/10 \text{ ms} \qquad (6.4) \\ &\leqq 0.33 \text{ ms} \end{aligned}$$

Finally, the displacement was taken to be applied at node 1 of the finite element model, consistent with the source of the acceleration record.

As MSC/pal uses the modal superposition method to compute transient response, the modes to use must be specified. In the present work, modes 1, 3, 4, 5, and 6 were chosen, mode 2 being eliminated due to its questionable accuracy (see Chap. 4, Model Verification).

All of the above are summarized in the command file listing, Appendix 5. Note that in the command file listing, displacement of node 15 is to be plotted as well as node 1, and this is discussed in Chap. 7, Results and Discussion. Note also that in the model specification (see Appendix 3), the ANALYZE command as used restricts the force and moment analysis to node 39, and this is also discussed in Chap. 7.

Chapter 7: RESULTS AND DISCUSSION

Figure 7.1 shows the resulting displacements of nodes 1 (curve A) and 15 (curve B) and Appendix 12 gives the corresponding discrete values. Curve A, of course, is simply the plot of input data, and one can compare it to Fig. 6.5 of Chap. 6. Curve B, however, is model dependent and is of interest as a check on model validity. Fig. 7.2 is a displacement curve for node 15 resulting from the second integration of Fig. 5.6 in Chap 5 (i.e., from the same loading event that curve A is derived from except now the acceleration history is used from node 15). Comparing curve B and Fig. 7.2, the amplitude match is not particularly good. Maximum displacements compare as

curve B: z_{max}=6.47 mm (0.255 in)

Figure 7.2: z_{max}=9.08 mm (0.358 in)

with about 29% difference. It is possible that the omission of mode 2 data in the analysis is responsible for lack of better agreement.

Appendix 9 shows the results of the transient analysis in terms of forces and moments at node 39 (the node just adjacent to the fixed node 40). It is assumed here that maximum stress will occur at node 39. For ideal cantilever bending, maximum stress occurs at the fixed end (node 40) but possible inaccuracies due to edge effects motivated the analysis at node 39. Maximum forces and moments are seen to occur at 4.0 ms and are shown on Fig. 7.3.

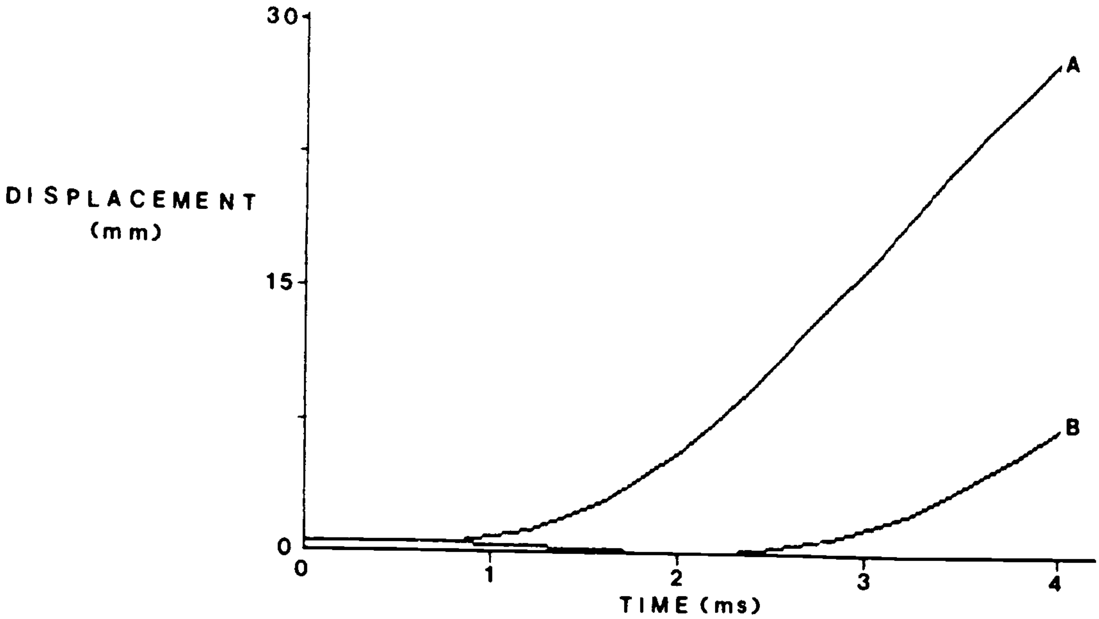

Figure 7.1. Transient analysis displacement results for nodes 1 and 15

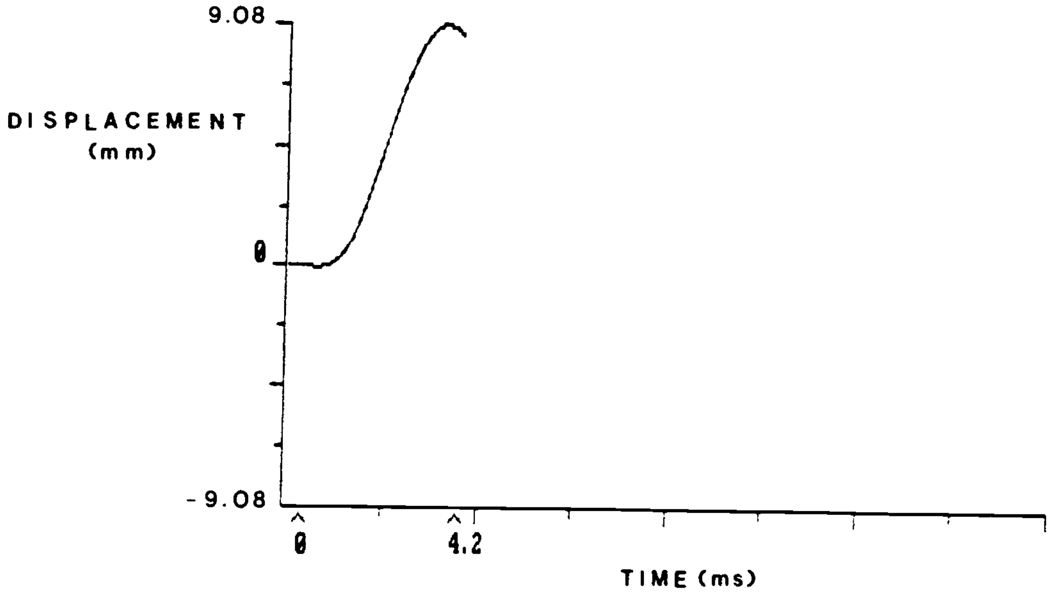

Figure 7.2. Displacement history for node 15 for central impact during dynamic loading based on double integration of acceleration history

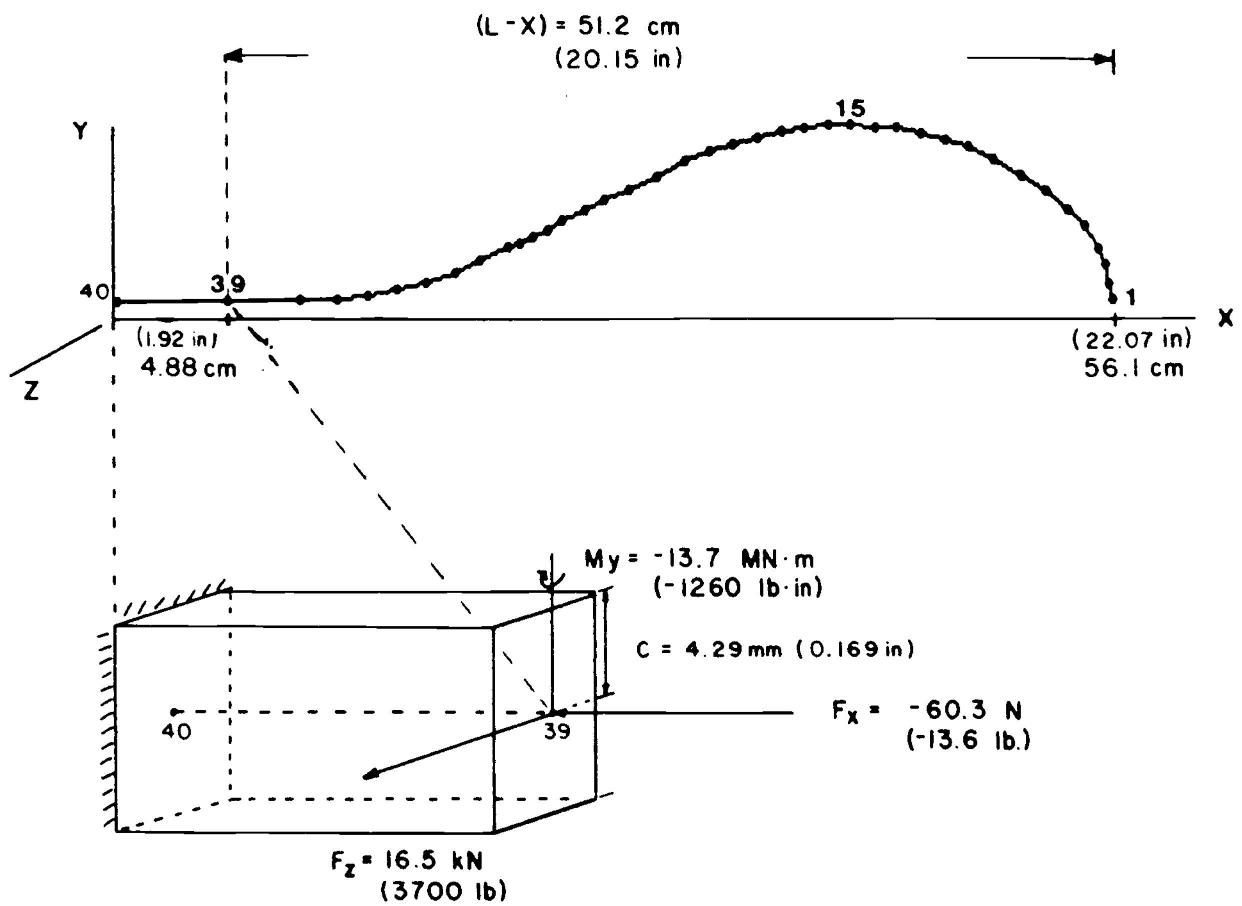

Figure 7.3. Transient analysis maximum force and moment results for node 39

A hand calculation (it was never discovered how to accomplish this in MSC/pal) of the maximum bending stress (disregarding shear effects) is given by the relation from elementary mechanics as

$$\sigma_x = Mc/I_{yy}$$
$$= 254 \text{ MPa } (36.8 \text{ ksi}).$$

Insight into this value may be gained by computing the stress of a simple, prismatic cantilever beam suddenly loaded, by a force P, to a maximum displacement of 26 mm (1.1 in), corresponding to the maximum deflection of node 1. The beam has the same geometrey, mass, and material properties as those of the racket, as shown in Fig 7.4.

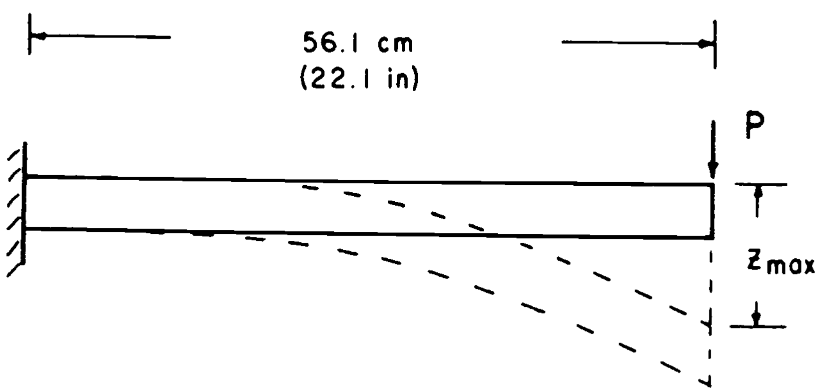

Figure 7.4. Equivalent cantilever beam suddenly loaded

A lower bound for the stress value can be found using the well-known result from technical mechanics (e.g., see Ugural & Fenster [1981], pg. 115) that, for a suddenly applied load P, the impact factor $1+\sqrt{[1+(2h/z_{st})]}$ may be taken as 2 (at h=0), or

$$P=2W \tag{7.1}$$

where P is the load required to cause the equivalent static displacement. Readily finding the deflection of a cantilever beam at its free end as

$$z_{max}=PL^3/3EI, \tag{7.2}$$

P is then

$$P=(3EI/L^3)z_{max}. \tag{7.3}$$

The bending moment at node 39 is given by

$$\begin{aligned} M&=P(L-x) \\ &= 2W(L-x). \end{aligned} \tag{7.4}$$

Then the maximum bending stress under dynamic loading is

$$\begin{aligned} \sigma_b&=Mc/I \\ &= P(L-x)c/I \\ &= (3EIz_{max}/L^3)(L-x)c/I \\ &=120 \text{ MPa } (10.3 \text{ ksi}). \end{aligned} \tag{7.5}$$

This result is a lower bound for the following two reasons: first, the suddenly applied loading condition (h=0) represents the lowest impact factor possible (for any $h>z_{st}$); second, deviations occur in the actual elastic curve from the assumed elastic curve (see ASME [1953], pg. 205).

Further light may be shed on the dynamic stress result by an energy consideration. The procedure is to consider the kinetic energy of the incident tennis ball as being transferred to the racket-holding fixture system. Our interest here is in that portion of the incident energy transformed into strain energy of the racket frame and the associated frame stress.

The strain energy in the racket frame is found from the work of the applied loads, which in the case of bending of a beam is given by (see Tauchert [1974], pg. 54):

$$U=\int_0^L (M^2/2EI)\,dx \;. \qquad (7.6)$$

For the equiv. beam , the moment is given by M=Px and the integral becomes

$$U=(1/2EI)\int_0^L (P^2x^2)\,dx \qquad (7.7)$$

$$=P^2L^3/6EI.$$

The strain energy of the racket frame is then set equal to the portion of the input kinetic energy, $1/2\ mv^2$, allotted to the frame, where m is the ball mass. For simplicity, this is accomplished as follows: the racket-holding fixture system is modeled as 3 springs in series, each subject to the same dynamic load but deflecting as a function of their individual stiffness. These stiffnesses are:

racket frame	k_f= 3.5 N/mm (20 lb/in)
mesh	k_m= 22.8 N/mm (130 lb/in)
holding fixture	k_h= 6.5 N/mm (37 lb/in)

Three springs in series have an equivalent stiffness, k_{eq}, found from

$$\frac{1}{k_{eq}} = \frac{1}{k_f} + \frac{1}{k_m} + \frac{1}{k_h} = 0.49 \text{ mm/N } (0.085 \text{ in/lb}) \qquad (7.8)$$

Then the frame's contribution to this stiffness is

$$(1/k_f)/(1/k_{eq})=(1/3.5)/0.49$$

$=0.59$ The strain energy of the racket frame is then allotted in the same proportion as the above ratio, i.e., 59% of the incident energy is frame strain energy (elastic potential energy varies directly as the stiffness). Then the strain energy of the frame becomes

$$U=P^2L^3/6EI=0.59(1/2)mv^2. \qquad (7.9)$$

Solving for P as (with m=W/g)

$$P=\sqrt{[(6/2)(0.59)(EI/L^3)(W/g)v^2]}$$

$$=242 \text{ N } (54.4 \text{ lb}).$$

The stress at node 39 is easily found then as

$$\sigma_b=P(L-x)c/I$$

$$=223 \text{ MPa } (32.2 \text{ ksi}).$$

This simple analysis gives agreement here that is quite satisfactory with the finite element bending stress previously given as 254 MPa (36.8 ksi).

To conclude this chapter, the assumptions under which this investigation took place are summarized:

1. Frame loading occurs at the mesh/frame attachment points.
2. Prismatic beam elements were used.

3. Contributions to frame damping by the mesh are negligible. Frame damping is negligible.
4. Frame bending for central hits occurs without torsion.
5. The cross section moments of inertia were the least precisely known frame parameters, and thus were candidates for variation during an iterative process to bring the f.e.m. model into compliance with experimental data.
6. Modes 1, 3, 4, 5 & 6 were sufficient for transient analysis.
7. A compliant testing fixture was more representative than either the fixed or free handle boundary condition.
8. Accelerometers instrumenting the racket did not appreciably affect the resulting dynamics.
9. Use of node 1 acceleration history data would give similar results to use of (say) node 15 data (or any other).
10. The displacement history (obtained from integrated acceleration history) could be used in lieu of the acceleration history.
11. The dynamic loading occurred only over an estimated ball dwell time of approximately 4 ms and the maximum frame bending stress occurred during this interval.
12. Maximum bending stress occurs near the frame fixed end.

Chapter 8: CONCLUSION

At first glance, a tennis racket seems to be a rather simple object. Made from familiar materials - metal, plastic, a leather handgrip - it is formed into familiar shapes. On closer inspection, however, the racket displays much greater complexity. Showing its true dynamical system nature, a symphony of interacting parts is revealed: the vibration modes and associated material response of the deformed frame, the deformation characteristics of the mesh, and the mesh - frame interaction as load is transferred from mesh to frame then back again.

In the present work, one small score from that symphony has been analyzed. A method has been developed to determine the dynamic stress in a tennis racket frame under loading conditions simulating tennis play. A finite element model was developed and then modified to comply with experimental data. Dynamic loading data was then experimentally determined. Results of the subsequent transient analysis show good agreeement with analytically derived values. As the loading more closely matches that of actual play, one may have more confidence that the computed frame stress approaches the actual stress. Then one may decide if the frame design is optimum in the sense of a fully stressed design.

Chapter 9: FUTURE DIRECTIONS

As shown in Chapter 7, Results and Discussion, many simplifying assumptions have been used in the present analysis. In that regard and to those wishing to carry the analysis further, the following future directions are offered.

1. Add in torsional d.o.f. to the f.e.m. model and remove for dynamic analysis by using the eigenvalue economizer method. This might give a torsion mode in one of the lower modes of vibration.
2. With a larger capacity f.e.m. program, include in the model the mesh directly as strut elements.
3. Include mode 2 in the transient analysis.
4. Develop a spring (or ?) assisted testing fixture to swing the racket into the ball.
5. Use the acceleration history data directly as input (rather than displacement history data).
6. Use (say) node 15 acceleration history data as input into the transient anlysis and compare to previous results at node 39.
7. Verify that maximum stress occurs near the frame fixed end.
8. Use mode shapes to verify the 'sweet spot' (center of percussion) location by determining nodal points.

CHAPTER 10: BIBLIOGRAPHY

ASME Handbook:Metals Engineering-Design. New York:American Society of Mechanical Engineers, 1953.

Avriel, M., Rychaert, M.J. and Wilde, D.J. (eds.), Optimization and Design. New Jersey:Prentice-Hall, 1971.

Baker, J.A., and Putnam, C.A., "Tennis Racket and Ball Responses During Impact Under Clamped and Freestanding Conditions." Research Quarterly 50(2), 1979, pp. 164-170.

Baker, J.A., and Wilson, B.D., "The Effect of Tennis Racket Stiffness and String Tension on Ball Velocity After Impact," Research Quarterly 49(3), 1978, pp. 255-259.

Brody, H., "Physics of the Tennis Racket," Am. J. Phys. 47(6), June 1979, pp. 482-487.

Blue Feather Software, Madison, Wisc., 1987.

Clough, R.W. and Penzien, J., Dynamics of Structures. New York:McGraw Hill, 1975.

Crowley, E.M., "The Historical Development of the Tennis Racket with Special Reference to United States Patents, 1836-1975," B.S. Thesis, Skidmore College, 1976.

Dawe, D.J., Matrix and Finite Element Displacement Analysis of Structures. London: Oxford University Press, 1983.

Ebert, L., "Materials in Sports-A New Undergraduate Course in Engineering," Machine Design, August 1976, pp. 18-23.

Ebhart, R., "The Influence of Modeling Techniques on Natural Frequency Predictions," ANSYS Users Conference Proceedings, Swanson Analysis Systems, Inc., 1987.

Elliot, B.C., Blanksby, B.A., and Ellis, R., "Vibration and Rebound Velocity Characteristics of Conventional and Oversized Tennis Rackets," Reserch Quarterly for Exercise and Sport 51(4), 1980, pp. 608-615.

Elliot, B., "The Influence of Tennis Racket Flexibility and String Tension on Rebound Velocity Following a Dynamic Impact," Research Quarterly for Exercise and Sport 53(4), 1982, pp. 277-281.

Fiott, S., Tennis Equipment. Pennsylvania:Chilton Book Co., 1978.

Floyd, C.G., "The Determination of Stress Using a Combined Theoretical and Experimental Analysis Approach," in Brebbia, C.A., and Keramidas, G.A. (eds.), Computational Methods and Experimental Measurements. New York:Springer-Verlay, 1984.

Freund, H., Unpublished research, Oregon State University, 1986.

Gallagher, R.H., and Zienkiewicz, O.C. (eds.), Optimum Structural Design. London:John Wiley & Sons, 1973.

Hatze, H., Forces and Duration of Impact, and Grip Tightness During the Tennis Stroke," Medicine and Science in Sports and Exercise 8(2), 1976, pp. 98-95.

Kane, T.R., Hayes, W.C., and Priest, J.D., "Experimental Determination of Forces Exerted in Tennis Play," in Nelson, R.C., and Morehouse, C.A. (eds.), Biomechanics IV. Baltimore:University Park Press, 1974, pp. 285-290.

Kollbrunner, C.F., and Basler, K., Torsion in Structures, an Engineering Approach. New York:Springer-Verlay, 1969.

Lai, H., "Machine Structure Refinement Using FEM and Experimental Techniques," ASME Design Engineering Technical Conference, Columbus, Ohio, October 1986.

Liu, Y.K., "Mechanical Analysis of Racket and Ball During Impact," Medicine and Science in Sports and Exercise 15(5), 1983, pp. 388-392.

MSC/pal, MacNeal-Schwendler Corp., 1984.

NAGWS Tennis Guide-Official Rules, National Association for Girls and Women in Sports, 1986.

Omichi, H., Miyashita, M., and Mizuno, T., "Bending Forces Acting on the Racquet During the Tennis Stroke," in Terauds, J. (ed.), Science in Racquet Sports:Science in Sports. Del Mar:Academic Publisher, 1979, pp. 89-95.

Plagenhoef, S., "Tennis Racket Testing," in Terauds, J. (ed.), Biomechanics in Sports. Del Mar:Research Center for Sports, 1982, pp. 411-421.

Rao, S., The Finite Element Method in Engineering. New York:Pergamon, 1982.

Steele, J., "Calibrating the Accuracy of Finite Element Calculations," ANSYS Users Conference Proceedings, Swanson Analysis Systems, Inc., 1987.

Tauchert, T.R., Energy Principles in Structural Mechanics. New York:McGraw-Hill, 1974.

Thomson, W.T., Theory of Vibration with Applications, 2nd ed. New Jersey:Prentice-Hall, Inc., 1981.

Ugural, A.C., and Fenster, S.K., Advanced Strength and Applied Elasticity. New York:Elsevier Science Publishing, 1981.

APPENDICIES

Appendix 1: Properties of 7005 aluminum

7005
4.6Zn-1.4Mg-0.5Mn-0.1Cr-0.1Zr-0.03Ti

Specifications

ASTM. Extruded wire, rod, bar, shapes and tube: B221
UNS number. A97005

Chemical Composition

Composition limits. 0.10 max Cu; 1.0 to 1.8 Mg; 0.20 to 0.70 Mn; 0.35 max Si; 0.40 max Fe; 0.06 to 0.20 Cr; 0.01 to 0.06 Ti; 4.0 to 5.0 Zn; 0.08 to 0.20 Zr; 0.05 max others (each); 0.15 max others (total); rem Al

Applications

Typical uses. Extruded structural members such as frame rails, cross members, corner posts, side posts and stiffeners for trucks, trailers, cargo containers and rapid transit cars. Welded or brazed assemblies requiring moderately high strength and high fracture toughness, such as large heat exchangers, especially where solution heat treatment after joining is impractical. Sports equipment such as tennis racquets and softball bats

Precautions in use. To avoid stress corrosion cracking, stresses in the transverse direction should be avoided at exposed machined or sawed surfaces. Parts should be cold formed in O temper, then heat treated; alternatively, parts may be cold formed in W temper, followed by artificial aging. In parts intended for service in aggressive electrolytes such as seawater, selective attack along the heat affected zone in a weldment or torch-brazed assembly can be avoided by postweld aging. When the service environment is conducive to galvanic corrosion, 7005 should be coupled or joined only to aluminum alloy components having similar electrolytic solution potentials; alternatively, joint surface should be protected or insulated.

Mechanical Properties

Tensile properties. Typical. Tensile strength: O temper, 193 MPa (28 ksi); T53 temper, 393 MPa (57 ksi); T6, T63, T6351 tempers, 372 MPa (54 ksi). Yield strength: O temper, 83 MPa (12 ksi); T53 temper, 345 MPa (50 ksi); T6, T63, T6351 tempers, 317 MPa (46 ksi). Elongation in 2 in. or 4 *d*, where *d* is diameter of tensile test specimen: O temper, 20%; T53 temper, 15%; T6, T63, T6351 tempers, 12%. See also Tables 92 and 93.

Shear strength. Typical. O temper: 117 MPa (17 ksi); T53 temper: 221 MPa (32 ksi); T6, T63, T6351 tempers: 214 MPa (31 ksi); see also Table 92.

Compressive strength. See Table 92.

Elastic modulus. Tension, 71 GPa (10.3×10^6 psi); shear, 26.9 GPa (3.9×10^6 psi); compression, 72.4 GPa (10.5×10^6 psi)

Fatigue strength. Rotating beam at 10^8 cycles. T6351 plate: smooth specimens, 115 to 130 MPa (17 to 19 ksi); 60° notched specimens, 20 to 50 MPa (3 to 7 ksi). T53 extrusions: smooth specimens, 130 to 150 MPa (19 to 22 ksi); 60° notched specimens, 24 to 40 MPa (3.5 to 6 ksi). Axial ($R = 0$) at 10^8 cycles, smooth specimens. T6351 plate: 195 MPa (28 ksi). T53 extrusions: 231 MPa (33.5 ksi)

Plane-strain fracture toughness. Typical, T6351 temper. LT orientation: 51.3 MPa$\sqrt{m}$ (46.7 ksi$\sqrt{in.}$); data from 3 in. thick notch bend specimens. TL orientation: 44 MPa$\sqrt{m}$ (40 ksi$\sqrt{in.}$); data from 3 in. thick notch bend specimens. SL orientation: 30.3 MPa$\sqrt{m}$ (27.6 ksi$\sqrt{in.}$); data from 1 to 1¼ in. thick compact tensile specimens.

Mass Characteristics

Density. 2.78 Mg/m^3 (0.100 lb/in.^{3}) at 20 °C (68 °F)

Appendix 1: (con't)

Table 92 Minimum mechanical properties of alloy 7005

Temper	Tensile strength MPa	Tensile strength ksi	Yield strength MPa	Yield strength ksi	Elongation(a), %	Compressive yield strength MPa	Compressive yield strength ksi	Shear strength MPa	Shear strength ksi	Shear yield strength MPa	Shear yield strength ksi
Extrusions											
T53											
L direction	345	50	303	44	10	296	43	193	28	172	25
LT direction	331	48	290	42	...	303	44	...	...	...	...

(a) In 2 in. or 4*d*, where *d* is diameter of reduced section of tensile test specimen.

Table 93 Typical tensile properties at various temperatures for alloy 7005-T53 extrusions

Temperature °C	Temperature °F	Tensile strength(a) MPa	Tensile strength(a) ksi	Yield strength(a) MPa	Yield strength(a) ksi	Elongation, %
−269	−452	641	93	483	70	16
−196	−320	538	78	421	61	16
−80	−112	441	64	379	55	13
−28	−18	421	61	359	52	14
24	75	392	57	345	50	15
100	212	303	44	283	41	20
149	300	165	24	145	21	35
204	400	97	14	83	12	60
260	500	76	11	66	9.5	80

(a) Lowest strength for exposures up to 10 000 h at temperature, no load; test loading applied at 5000 psi/min to yield strength and then at strain rate of 5%/min to fracture.

Appendix 2: Forty-two node model definition file

```
TITLE  FEM TENNIS RACKET ANALYSIS - 42 node model
NODAL POINT LOCATIONS
1,22.07,.25,0
2,22.02,.613,0
3,21.93,1.05,0
4,21.80,1.47,0
5,21.55,1.96,0
6,21.21,2.34,0
7,20.78,2.77,0
8,20.3,3.15,0
9,19.71,3.54,0
10,19.23,3.78,0
11,18.75,3.98,0
12,18.26,4.12,0
13,17.77,4.22,0
14,17.34,4.27,0
15,16.84,4.32,0
16,16.41,4.32,0
17,15.93,4.27,0
18,15.44,4.17,0
19,14.95,4.03,0
20,14.47,3.88,0
21,13.99,3.74,0
22,13.49,3.47,0
23,12.89,3.15,0
24,12.34,2.86,0
25,11.84,2.59,0
26,11.44,2.38,0
27,10.99,2.14,0
28,10.69,1.98,0
29,10.39,1.82,0
30,10.14,1.68,0
31,9.89,1.55,0
32,9.34,1.26,0
33,8.84,0.99,0
34,8.24,0.76,0
35,7.64,0.60,0
36,7.04,0.49,0
37,6.42,0.43,0
38,5.72,0.42,0
39,4.92,0.42,0
40,3.92,0.42,0
41,2.92,0.42,0
42,1.92,0.42,0

MATERIAL 10.3E6,3.8E6,2.54E-4,0.334
BEAM TYPE 1,0.166,1.5E-3,4.94E-3,8.81E-4
CON 1 TO 2
CON 2 TO 3
CON 3 TO 4
CON 4 TO 5
CON 5 TO 6
CON 6 TO 7
CON 7 TO 8
CON 8 TO 9
CON 9 TO 10
CON 10 TO 11
CON 11 TO 12
CON 12 TO 13
CON 13 TO 14
CON 14 TO 15
CON 15 TO 16
CON 16 TO 17
CON 17 TO 18
CON 18 TO 19
CON 19 TO 20
CON 20 TO 21
CON 21 TO 22
CON 22 TO 23
CON 23 TO 24
CON 24 TO 25
CON 25 TO 26
CON 26 TO 27
CON 27 TO 28
CON 28 TO 29
CON 29 TO 30
CON 30 TO 31
CON 31 TO 32
CON 32 TO 33
CON 33 TO 34
CON 34 TO 35
CON 35 TO 36
CON 36 TO 37
CON 37 TO 38
CON 38 TO 39
CON 39 TO 40
CON 40 TO 41, ANALYZE
CON 41 TO 42

ZERO
ALL COMPONENTS OF 42
Y TRANSLATION OF ALL
X ROTATION OF ALL
Z ROTATION OF ALL

END DEFINITION
```

Appendix 3: Forty node model definition file

```
TITLE  FEM TENNIS RACKET ANALYSIS - 40 node model
NODAL POINT LOCATIONS
1,22.07,.25,0
2,22.02,.613,0
3,21.93,1.05,0
4,21.80,1.47,0
5,21.55,1.96,0
6,21.21,2.34,0
7,20.78.2.77,0
8,20.3,3.15,0
9,19.71,3.54,0
10,19.23,3.78,0
11,18.75,3.98,0
12,18.26,4.12,0
13,17.77,4.22,0
14,17.34,4.27,0
15,16.84,4.32,0
16,16.41,4.32,0
17,15.93,4.27,0
18,15.44,4.17,0
19,14.95,4.03,0
20,14.47,3.88,0
21,13.99,3.74,0
22,13.49,3.47,0
23,12.89,3.15,0
24,12.34,2.86,0
25,11.84,2.59.0
26,11.44,2.38,0
27,10.99,2.14.0
28,10.69,1.98.0
29,10.39,1.82,0
30,10.14,1.68,0
31,9.89.1.55,0
32,9.34.1.26.0
33,8.84,0.99,0
34,8.24,0.76.0
35.7.64,0.60,0
36,7.04,0.49,0
37,6.42,0.43.0
38,5.67,0.42,0
39,4.17,0.42.0
40,1.92,0.42.0
MATERIAL 10.3E6.3.8E6.2.54E-4.0.334
BEAM TYPE 1.0.166.1.5E-3.5.80E-3.8.50E-5
CON 1 TO 2
CON 2 TO 3
CON 3 TO 4
CON 4 TO 5
CON 5 TO 6
CON 6 TO 7
CON 7 TO 8
CON 8 TO 9
CON 9 TO 10
CON 10 TO 11
CON 11 TO 12
CON 12 TO 13
CON 13 TO 14
CON 14 TO 15
CON 15 TO 16
CON 16 TO 17
CON 17 TO 18
CON 18 TO 19
CON 19 TO 20
CON 20 TO 21
CON 21 TO 22
CON 22 TO 23
CON 23 TO 24
CON 24 TO 25
CON 25 TO 26
CON 26 TO 27
CON 27 TO 28
CON 28 TO 29
CON 29 TO 30
CON 30 TO 31
CON 31 TO 32
CON 32 TO 33
CON 33 TO 34
CON 34 TO 35
CON 35 TO 36
CON 36 TO 37
CON 37 TO 38
CON 38 TO 39, ANALYZE
CON 39 TO 40
ZERO
ALL COMPONENTS OF 40
Y TRANSLATION OF ALL
X ROTATION OF ALL
Z ROTATION OF ALL

END DEFINITION
```

Appendix 4: Accelerometer specifications

MINIATURE 2 GRAM

QUARTZ ACCELEROMETER
Series 303A

PCB PIEZOTRONICS

with built-in microelectronics & 10 mV/g sensitivity

Measure shock and vibration in applications requiring small size, low mass or very high frequency response.

Series 303A Quartz Accelerometers function to transfer shock and vibratory motion into high-level, low-impedance (100 ohm) voltage signals compatible with readout, recording or analyzing instruments. These tiny sensitive (10 mV/g) sensors operate reliably over wide amplitude and frequency ranges under adverse environmental conditions.

They are structured with permanently polarized compression-mode quartz elements and a microelectronic amplifier housed in a lightweight metal case. Three different case and connector configurations give you a choice in mounting and cabling. The built-in electronics operate over a coaxial or two-conductor cable; one lead conducts both signal and power. Solder terminal versions are normally supplied with a ribbon wire cable (10 ft. long; Model 007B10) attached. Model 303A02 requires Model 002G coaxial cable with a Micro 5-44 connector on one end.

Test results of the behavior of the Model 303A are presented below. Note especially the sharp clean signals free of cable noise and the exceptionally high frequency response. Because of the low mass, Series 303A sensors measure motion of many light structures without appreciably changing the structure or behavior of the test object during the measuring transaction.

Frequency Response (mounted)

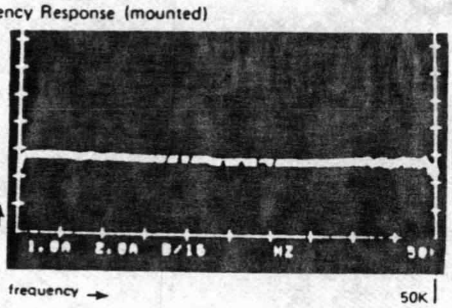

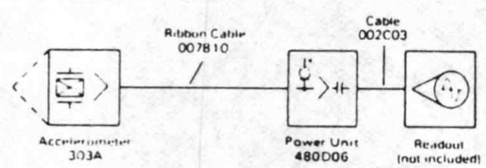

303A

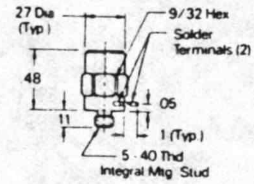

Supplied with attached 10' ribbon wire terminating in 10-32 Micro connector

303A02

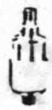

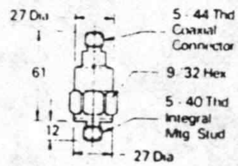

303A03

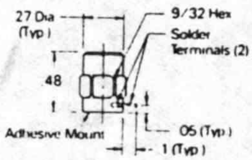

Supplied with attached 10' ribbon wire terminating in 10-32 Micro connector

SPECIFICATIONS: Model No.		303A & 303A03
Range (for ±5 output)	g	±500
Resolution	g	0.01
Sensitivity (nominal)	mV/g	10
Resonant Frequency (mounted)	kHz	70
Frequency Range (±5%)	Hz	1 to 10000
Discharge Time Constant	sec	1
Linearity	%	1
Output Impedance	ohm	100
Output Bias (nominal)	V	11
Overload Recovery	microsec	10
Transverse Sensitivity (max.)	%	5
Strain Sensitivity	g/μin/in	0.05
Temperature Coefficient	%/°F	0.03
Temperature Range (operational to +250°F)	°F	−40 to +200
Vibration	g	±1000
Shock (protected)	g	2000
Size (hex x height)	in	0.28 x 0.48
Weight (approx.)	gm	2
Connector (solder terminals)		2
Case Material		s.s.
Seal		epoxy
Excitation Voltage	V	+18 to 24
Excitation Current (constant)	mA	2 to 20

Notes:

Model 303A02 has a 5-44 micro connector. Other specifications are the same.

Options include 080A15 adhesive mounting base, 080A16 three-axis mounting adaptor (10-32 thread) and triaxial Model 303A06.

Appendix 5: Transient analysis input file

```
TITLE DISPLACEMENT LOADING
TIME 0.0042,0.0002
DISPLACEMENT APPLIED
TZ 1, 0.0386

EXCITATION DEFINITION
0.0,0.0        0.0002,0.0     0.0004,0.0     0.0006,0.0146  0.0008,0.102
0.001,0.366    0.0012,0.819   0.0014,1.54    0.0016,2.53    0.0018,3.83
0.002,5.35     0.0022,7.15    0.0024,9.15    0.0026,11.3    0.0028,13.6
0.003,15.8     0.0032,18.2    0.0034,20.6    0.0036,22.9    0.0038,25.2
0.0040,27.4    0.0042,0.0

USE MODES 1.3,4,5,6
PLOT DISP TZ 1,15
SOLVE
```

Appendix 6: Voltage vs time listings for frame damping

```
DISCRETE VOLTAGE vs TIME FOR RACKET IMPACT
T=  0        V=  .5795          X.
T=  0        V=  .5795 .8
T=  .8       V=  .581
T=  .8       V=  .581 1.6
T=  1.6      V=  .566
T=  1.6      V=  .566 2.4
T=  2.4      V=  .5495001
T=  2.4      V=  .5495001 3.2
T=  3.2      V=  .5240001
T=  3.2      V=  .5240001 4
T=  4        V=  .4895
T=  4        V=  .4895 4.8
T=  4.8      V=  .45
T=  4.8      V=  .45 5.6
T=  5.6      V=  .4155
T=  5.6      V=  .4155 6.4
T=  6.4      V=  .374
T=  6.4      V=  .374 7.2
T=  7.2      V=  .342
T=  7.2      V=  .342 8
T=  8        V=  .312
T=  8        V=  .312 8.8
T=  8.8      V=  .282
T=  8.8      V=  .282 9.6
T=  9.6      V=  .255
T=  9.6      V=  .255 10.4
T=  10.4     V=  .222
T=  10.4     V=  .222 11.2
T=  11.2     V=  .1845
T=  11.2     V=  .1845 12
T=  12       V=  .146
T=  12       V=  .146 12.8
T=  12.8     V=  .114
T=  12.8     V=  .114 13.6
T=  13.6     V=  .0855
T=  13.6     V=  .0855 14.4
T=  14.4     V=   7.600001E-02
T=  14.4     V=   7.600001E-02 15.2
T=  15.2     V=  .0645
T=  15.2     V=  .0645 16
T=  16       V=  .047
T=  16       V=  .047 16.8
T=  16.8     V=  .035
T=  16.8     V=  .035 17.6
T=  17.6     V=  .028
T=  17.6     V=  .028 18.4
T=  18.4     V=  .041
T=  18.4     V=  .041 19.2
T=  19.2     V=   7.650001E-02
T=  19.2     V=   7.650001E-02 20
T=  20       V=  .1155
T=  20       V=  .1155 20.8
T=  20.8     V=  .147
T=  20.8     V=  .147 21.6
T=  21.6     V=  .17
T=  21.6     V=  .17 22.4
T=  22.4     V=  .1845
T=  22.4     V=  .1845 23.2
T=  23.2     V=  .2155
T=  23.2     V=  .2155 24
T=  24       V=  .2675
T=  24       V=  .2675 24.8
T=  24.8     V=  .322
T=  24.8     V=  .322 25.6
T=  25.6     V=  .3725
T=  25.6     V=  .3725 26.4
T=  26.4     V=  .4055
T=  26.4     V=  .4055 27.2
T=  27.2     V=  .422
T=  27.2     V=  .422 28
T=  28       V=  .434
T=  28       V=  .434 28.8
T=  28.8     V=  .457
T=  28.8     V=  .457 29.6
T=  29.6     V=  .4815
T=  29.6     V=  .4815 30.4
T=  30.4     V=  .516
T=  30.4     V=  .516 31.2
```

Appendix 6: (con't)

```
T=  [illegible]     V=  [illegible]
T=  32        V=  .5625
T=  32        V=  .5625 32.8
T=  32.8        V=  .5725001        7.
T=  32.8        V=  .5725001 33.6
T=  33.6        V=  .572
T=  33.6        V=  .572 34.4
T=  34.4        V=  .565
T=  34.4        V=  .565 35.2
T=  35.2        V=  .546
T=  35.2        V=  .546 36
T=  36        V=  .525
T=  36        V=  .525 36.8
T=  36.8        V=  .5005
T=  36.8        V=  .5005 37.6
T=  37.6        V=  .4715
T=  37.6        V=  .4715 38.4
T=  38.4        V=  .4365
T=  38.4        V=  .4365 39.2
T=  39.2        V=  .404
T=  39.2        V=  .404 40
T=  40        V=  .3645
T=  40        V=  .3645 40.8
T=  40.8        V=  .326
T=  40.8        V=  .326 41.6
T=  41.6        V=  .295
T=  41.6        V=  .295 42.4
T=  42.4        V=  .2575
T=  42.4        V=  .2575 43.2
T=  43.2        V=  .219
T=  43.2        V=  .219 44
T=  44        V=  .187
T=  44        V=  .187 44.8
T=  44.8        V=  .1605
T=  44.8        V=  .1605 45.6
T=  45.6        V=  .1335
T=  45.6        V=  .1335 46.4
T=  46.4        V=  .113
T=  46.4        V=  .113 47.2
T=  47.2        V=  .0895
T=  47.2        V=  .0895 48
T=  48        V=  7.250001E-02
T=  48        V=  7.250001E-02 48.8
T=  48.8        V=  .064
T=  48.8        V=  .064 49.6
T=  49.6        V=  .066
T=  49.6        V=  .066 50.4
T=  50.4        V=  .0755
T=  50.4        V=  .0755 51.2
T=  51.2        V=  .0855
T=  51.2        V=  .0855 52
T=  52        V=  8.800001E-02
T=  52        V=  8.800001E-02 52.8
T=  52.8        V=  .0895
T=  52.8        V=  .0895 53.6
T=  53.6        V=  .1015
T=  53.6        V=  .1015 54.4
T=  54.4        V=  .131
T=  54.4        V=  .131 55.2
T=  55.2        V=  .179
T=  55.2        V=  .179 56
T=  56        V=  .232
T=  56        V=  .232 56.8
T=  56.8        V=  .2695
T=  56.8        V=  .2695 57.6
T=  57.6        V=  .297
T=  57.6        V=  .297 58.4
T=  58.4        V=  .323
T=  58.4        V=  .323 59.2
T=  59.2        V=  .352
T=  59.2        V=  .352 60
T=  60        V=  .3875
T=  60        V=  .3875 60.8
T=  60.8        V=  .4385
T=  60.8        V=  .4385 61.6
T=  61.6        V=  .4735
T=  61.6        V=  .4735 62.4
T=  62.4        V=  .4965
T=  62.4        V=  .4965 63.2
T=  63.2        V=  .5115
T=  63.2        V=  .5115 64
T=  64        V=  .5195
T=  64        V=  .5185 64.8
T=  64.8        V=  .5235
T=  64.9        V=  .5235 65.60001
T=  65.60001        V=  .5355001
T=  65.60001        V=  .5355001 66.40002
```

Appendix 6: (con't)

```
T=  66.40002      V=  .5415 67.20002
T=  67.20002      V=  .5315
T=  67.20002      V=  .5315 68.00002
T=  68.00002      V=  .528
T=  68.00002      V=  .528 68.80003
T=  68.80003      V=  .52
T=  68.80003      V=  .52 69.60004
T=  69.60004      V=  .5025
T=  69.60004      V=  .5025 70.40004
T=  70.40004      V=  .4825
T=  70.40004      V=  .4825 71.20004
T=  71.20004      V=  .4555
T=  71.20004      V=  .4555 72.00005
T=  72.00005      V=  .4205
T=  72.00005      V=  .4205 72.80006
T=  72.80006      V=  .384
T=  72.80006      V=  .384 73.60006
T=  73.60006      V=  .3465
T=  73.60006      V=  .3465 74.40006
T=  74.40006      V=  .306
T=  74.40006      V=  .306 75.20007
T=  75.20007      V=  .276
T=  75.20007      V=  .276 76.00008
T=  76.00008      V=  .244
T=  76.00008      V=  .244 76.80008
T=  76.80008      V=  .2095
T=  76.80008      V=  .2095 77.60008
T=  77.60008      V=  .1705
T=  77.60008      V=  .1705 78.40009
T=  78.40009      V=  .1365
T=  78.40009      V=  .1365 79.2001
T=  79.2001       V=  .105
T=  79.2001       V=  .105 80.00011
T=  80.00011      V=  .0935
T=  80.00011      V=  .0935 80.80011
T=  80.80011      V=  9.100001E-02
T=  80.80011      V=  9.100001E-02 81.60011
T=  81.60011      V=  8.800001E-02
T=  81.60011      V=  8.800001E-02 82.40012
T=  82.40012      V=  .086
T=  82.40012      V=  .086 83.20013
T=  83.20013      V=  .083
T=  83.20013      V=  .083 84.00013
T=  84.00013      V=  .0815
T=  84.00013      V=  .0815 84.80013
T=  84.80013      V=  9.100001E-02
T=  84.80013      V=  9.100001E-02 85.60014
T=  85.60014      V=  .113
T=  85.60014      V=  .113 86.40015
T=  86.40015      V=  .1355
T=  86.40015      V=  .1355 87.20015
T=  87.20015      V=  .1575
T=  87.20015      V=  .1575 88.00015
T=  88.00015      V=  .179
T=  88.00015      V=  .179 88.80016
T=  88.80016      V=  .1965
T=  88.80016      V=  .1965 89.60017
T=  89.60017      V=  .227
T=  89.60017      V=  .227 90.40017
T=  90.40017      V=  .269
T=  90.40017      V=  .269 91.20017
T=  91.20017      V=  .3145
T=  91.20017      V=  .3145 92.00018
T=  92.00018      V=  .355
T=  92.00018      V=  .355 92.80019
T=  92.80019      V=  .391
T=  92.80019      V=  .391 93.6002
T=  93.6002       V=  .414
T=  93.6002       V=  .414 94.4002
T=  94.4002       V=  .437
T=  94.4002       V=  .437 95.2002
T=  95.2002       V=  .464
T=  95.2002       V=  .464 96.00021
T=  96.00021      V=  .486
T=  96.00021      V=  .486 96.80022
T=  96.80022      V=  .507
T=  96.80022      V=  .507 97.60022
T=  97.60022      V=  .5235
[illegible]
T=  99.20023      V=  .5265001 100.0002 ← I₂
T=  100.0002      V=  .522
T=  100.0002      V=  .522 100.8002
T=  100.8002      V=  .5135
T=  100.8002      V=  .5135 101.6002
T=  101.6002      V=  .504
T=  101.6002      V=  .504 102.4002
```

Appendix 6: (con't)

T= 102.4002	V= [illegible]	103.2002	
T= 103.2002	V= .4695		
T= 103.2002	V= .4695	104.0002	
T= 104.0002	V= .442		
T= 104.0002	V= .442	104.8002	
T= 104.8002	V= .415		
T= 104.8002	V= .415	105.6002	
T= 105.6002	V= .3895		
T= 105.6002	V= .3895	106.4002	
T= 106.4002	V= .3605		
T= 106.4002	V= .3605	107.2002	
T= 107.2002	V= .3345		
T= 107.2002	V= .3345	108.0002	
T= 108.0002	V= .2985		
T= 108.0002	V= .2985	108.8002	
T= 108.8002	V= .2625		
T= 108.8002	V= .2625	109.6002	
T= 109.6002	V= .2245		
T= 109.6002	V= .2245	110.4002	
T= 110.4002	V= .1905		
T= 110.4002	V= .1905	111.2002	
T= 111.2002	V= .1665		
T= 111.2002	V= .1665	112.0002	
T= 112.0002	V= .145		
T= 112.0002	V= .145	112.8002	
T= 112.8002	V= .1245		
T= 112.8002	V= .1245	113.6002	
T= 113.6002	V= .103		
T= 113.6002	V= .103	114.4002	
T= 114.4002	V= .09		
T= 114.4002	V= .09	115.2002	
T= 115.2002	V= .082		
T= 115.2002	V= .082	116.0002	
T= 116.0002	V= .086		
T= 116.0002	V= .086	116.8002	
T= 116.8002	V= 9.500001E-02		
T= 116.8002	V= 9.500001E-02	117.6002	
T= 117.6002	V= .1065		
T= 117.6002	V= .1065	118.4002	
T= 118.4002	V= .1135		
T= 118.4002	V= .1135	119.2002	
T= 119.2002	V= .129		
T= 119.2002	V= .129	120.0002	
T= 120.0002	V= .151		
T= 120.0002	V= .151	120.8002	
T= 120.8002	V= .178		
T= 120.8002	V= .178	121.6002	
T= 121.6002	V= .2145		
T= 121.6002	V= .2145	122.4002	
T= 122.4002	V= .248		
T= 122.4002	V= .248	123.2002	
T= 123.2002	V= .2755		
T= 123.2002	V= .2755	124.0002	
T= 124.0002	V= .2965		
T= 124.0002	V= .2965	124.8002	
T= 124.8002	V= .323		
T= 124.8002	V= .323	125.6002	
T= 125.6002	V= .356		
T= 125.6002	V= .356	126.4002	
T= 126.4002	V= .3935		
T= 126.4002	V= .3935	127.2002	
T= 127.2002	V= .431		
T= 127.2002	V= .431	128.0002	
T= 128.0002	V= .4615		
T= 128.0002	V= .4615	128.8002	
T= 128.8002	V= .4765		
T= 128.8002	V= .4765	129.6002	
T= 129.6002	V= .486		
T= 129.6002	V= .486	130.4002	
T= 130.4002	V= .495		
T= 130.4002	V= .495	131.2002	
T= 131.2002	V= .5045		
T= 131.2002	V= .5045	132.0002	
T= 132.0002	V= .5165		
T= 132.0002	V= .5165	132.8002	
T= 132.8002	V= .5245		I_4
T= 132.8002	V= .5245	133.6002	
T= 133.6002	V= .5205		
T= 133.6002	V= .5205	134.4002	
T= 134.4002	V= .5075001		
T= 134.4002	V= .5075001	135.2002	
T= 135.2002	V= .485		
T= 135.2002	V= .485	136.0002	
T= 136.0002	V= .462		
T= 136.0002	V= .462	136.8002	
T= 136.8002	V= .4405		
T= 136.8002	V= .4405	137.6002	

Appendix 6: (con't)

T= 137.6002	V= .417	138.4002	
T= 138.4002	V= .391		
T= 138.4002	V= .391	139.2002	
T= 139.2002	V= .36		
T= 139.2002	V= .36	140.0002	
T= 140.0002	V= .326		
T= 140.0002	V= .326	140.8002	
T= 140.8002	V= .293		
T= 140.8002	V= .293	141.6002	
T= 141.6002	V= .2675		
T= 141.6002	V= .2675	142.4002	
T= 142.4002	V= .2435		
T= 142.4002	V= .2435	143.2002	
T= 143.2002	V= .2155		
T= 143.2002	V= .2155	144.0002	
T= 144.0002	V= .186		
T= 144.0002	V= .186	144.8002	
T= 144.8002	V= .1595		
T= 144.8002	V= .1595	145.6002	
T= 145.6002	V= .1355		
T= 145.6002	V= .1355	146.4002	
T= 146.4002	V= .122		
T= 146.4002	V= .122	147.2002	
T= 147.2002	V= .114		
T= 147.2002	V= .114	148.0002	
T= 148.0002	V= .11		
T= 148.0002	V= .11	146.8002	
T= 148.8002	V= .103		
T= 148.8002	V= .103	149.6002	
T= 149.6002	V= .0975		
T= 149.6002	V= .0975	150.4002	
T= 150.4002	V= .1015		
T= 150.4002	V= .1015	151.2002	
T= 151.2002	V= .1135		
T= 151.2002	V= .1135	152.0002	
T= 152.0002	V= .1355		
T= 152.0002	V= .1355	152.8002	
T= 152.8002	V= .159		
T= 152.8002	V= .159	153.6002	
T= 153.6002	V= .1805		
T= 153.6002	V= .1805	154.4002	
T= 154.4002	V= .2015		
T= 154.4002	V= .2015	155.2002	
T= 155.2002	V= .226		
T= 155.2002	V= .226	156.0002	
T= 156.0002	V= .257		
T= 156.0002	V= .257	156.8002	
T= 156.8002	V= .295		
T= 156.8002	V= .295	157.6002	
T= 157.6002	V= .3345		
T= 157.6002	V= .3345	158.4002	
T= 158.4002	V= .366		
T= 158.4002	V= .366	159.2002	
T= 159.2002	V= .3885		
T= 159.2002	V= .3885	160.0002	
T= 160.0002	V= .408		
T= 160.0002	V= .408	160.8002	
T= 160.8002	V= .428		
T= 160.8002	V= .428	161.6002	
T= 161.6002	V= .451		
T= 161.6002	V= .451	162.4002	
T= 162.4002	V= .4765		
T= 162.4002	V= .4765	163.2002	
T= 163.2002	V= .4965		
T= 163.2002	V= .4965	164.0002	
T= 164.0002	V= .5085		
T= 164.0002	V= .5085	164.8002	
T= 164.8002	V= .5095		I_s
T= 164.8002	V= .5095	165.6002	
T= 165.6002	V= .5045		
T= 165.6002	V= .5045	166.4002	
T= 166.4002	V= .4975		
T= 166.4002	V= .4975	167.2002	
T= 167.2002	V= .491		
T= 167.2002	V= .491	168.0002	
T= 168.0002	V= .4845		
T= 168.0002	V= .4845	168.8002	
T= 168.8002	V= .4725		
T= 168.9002	V= .4725	169.6002	
T= 163.6002	V= .4525		
T= 169.6002	V= .4525	170.4002	
T= 170.4002	V= .424		
T= 170.4002	V= .424	171.2002	
T= 171.2002	V= .392		
T= 171.2002	V= .392	172.0002	
T= 172.0002	V= .362		
T= 172.0002	V= .362	172.8002	

Appendix 6: (con't)

T=	[illegible]	V=	[illegible]	[illegible]	
T=	173.6002	V=	.304		
T=	173.6002	V=	.304	174.4002	
T=	174.4002	V=	.272		
T=	174.4002	V=	.272	175.2002	
T=	175.2002	V=	.24		
T=	175.2002	V=	.24	176.0002	
T=	176.0002	V=	.212		
T=	176.0002	V=	.212	176.8002	
T=	176.8002	V=	.188		
T=	176.8002	V=	.188	177.6002	
T=	177.6002	V=	.1705		
T=	177.6002	V=	.1705	178.4002	
T=	178.4002	V=	.1545		
T=	178.4002	V=	.1545	179.2002	
T=	179.2002	V=	.1385		
T=	179.2002	V=	.1385	180.0002	
T=	180.0002	V=	.124		
T=	180.0002	V=	.124	180.8002	
T=	180.8002	V=	.1135		
T=	180.8002	V=	.1135	181.6002	
T=	181.6002	V=	.106		
T=	181.6002	V=	.106	182.4002	
T=	182.4002	V=	.1125		
T=	182.4002	V=	.1125	183.2002	
T=	183.2002	V=	.1235		
T=	183.2002	V=	.1235	184.0002	
T=	184.0002	V=	.1345		
T=	184.0002	V=	.1345	184.8002	
T=	184.8002	V=	.143		
T=	184.8002	V=	.143	185.6002	
T=	185.6002	V=	.154		
T=	185.6002	V=	.154	186.4002	
T=	186.4002	V=	.1705		
T=	186.4002	V=	.1705	187.2002	
T=	187.2002	V=	.196		
T=	187.2002	V=	.196	188.0002	
T=	188.0002	V=	.2315		
T=	188.0002	V=	.2315	188.8002	
T=	188.8002	V=	.264		
T=	188.8002	V=	.264	189.6002	
T=	189.6002	V=	.292		
T=	189.6002	V=	.292	190.4002	
T=	190.4002	V=	.3155		
T=	190.4002	V=	.3155	191.2002	
T=	191.2002	V=	.3405		
T=	191.2002	V=	.3405	192.0002	
T=	192.0002	V=	.3685		
T=	192.0002	V=	.3685	192.8002	
T=	192.8002	V=	.4		
T=	192.8002	V=	.4	193.6002	
T=	193.6002	V=	.43		
T=	193.6002	V=	.43	194.4002	
T=	194.4002	V=	.4525		
T=	194.4002	V=	.4525	195.2002	
T=	195.2002	V=	.466		
T=	195.2002	V=	.466	196.0002	
T=	196.0002	V=	.475		
T=	196.0002	V=	.475	196.8002	
T=	196.8002	V=	.4815		
T=	196.8002	V=	.4815	197.6002	
T=	197.6002	V=	.491		
T=	197.6002	V=	.491	198.4002	
T=	198.4002	V=	.4995		
T=	198.4002	V=	.4995	199.2002	
T=	199.2002	V=	.4995		X.
T=	199.2002	V=	.4995	200.0002	
T=	200.0002	V=	.4895		
T=	200.0002	V=	.4895	200.8002	
T=	200.8002	V=	.4755		
T=	200.8002	V=	.4755	201.6002	
T=	201.6002	V=	.4585		
T=	201.6002	V=	.4585	202.4002	
T=	202.4002	V=	.4425		
T=	202.4002	V=	.4425	203.2002	
T=	203.2002	V=	.4265		
T=	203.2002	V=	.4265	204.0002	
T=	204.0002	V=	.4055		
T=	204.0002	V=	.4055	204.8002	
T=	204.8002	V=	.3795		
T=	204.8002	V=	.3795	205.6002	
T=	205.6002	V=	.3495		
T=	205.6002	V=	.3495	206.4002	
T=	206.4002	V=	.313		
T=	206.4002	V=	.313	207.2002	
T=	207.2002	V=	.284		
T=	207.2002	V=	.284	208.0002	

Appendix 6: (con't)

[illegible]	[illegible]		
T= 208.8002	V= .2335		
T= 208.8002	V= .2335 209.6002		
T= 209.6002	V= .208		
T= 209.6002	V= .208 210.4002		
T= 210.4002	V= .1825		
T= 210.4002	V= .1825 211.2002		
T= 211.2002	V= .1565		
T= 211.2002	V= .1565 212.0002		
T= 212.0002	V= .1385		
T= 212.0002	V= .1385 212.8002		
T= 212.8002	V= .126		
T= 212.8002	V= .126 213.6002		
T= 213.6002	V= .1205		
T= 213.6002	V= .1205 214.4002		
T= 214.4002	V= .12		
T= 214.4002	V= .12 215.2002		
T= 215.2002	V= .12		
T= 215.2002	V= .12 216.0002		
T= 216.0002	V= .12		
T= 216.0002	V= .12 216.8002		
T= 216.8002	V= .1245		
T= 216.8002	V= .1245 217.6002		
T= 217.6002	V= .1385		
T= 217.6002	V= .1385 218.4002		
T= 218.4002	V= .1595		
T= 218.4002	V= .1595 219.2002		
T= 219.2002	V= .183		
T= 219.2002	V= .183 220.0002		
T= 220.0002	V= .2045		
T= 220.0002	V= .2045 220.8002		
T= 220.8002	V= .2245		
T= 220.8002	V= .2245 221.6002		
T= 221.6002	V= .2455		
T= 221.6002	V= .2455 222.4002		
T= 222.4002	V= .2725		
T= 222.4002	V= .2725 223.2002		
T= 223.2002	V= .304		
T= 223.2002	V= .304 224.0002		
T= 224.0002	V= .3375		
T= 224.0002	V= .3375 224.8002		
T= 224.8002	V= .368		
T= 224.8002	V= .368 225.6002		
T= 225.6002	V= .3915		
T= 225.6002	V= .3915 226.4002		
T= 226.4002	V= .4095		
T= 226.4002	V= .4095 227.2002		
T= 227.2002	V= .4275		
T= 227.2002	V= .4275 228.0002		
T= 228.0002	V= .4485		
T= 228.0002	V= .4485 228.8002		
T= 228.8002	V= .469		
T= 228.8002	V= .469 229.6002		
T= 229.6002	V= .484		
T= 229.6002	V= .484 230.4002		
T= 230.4002	V= .4895	I_7	
T= 230.4002	V= .4895 231.2002		
T= 231.2002	V= .4885		
T= 231.2002	V= .4885 232.0002		
T= 232.0002	V= .4825		
T= 232.0002	V= .4825 232.8002		
T= 232.8002	V= .475		
T= 232.8002	V= .475 233.6002		
T= 233.6002	V= .4705		
T= 233.6002	V= .4705 234.4002		
T= 234.4002	V= .4605		
T= 234.4002	V= .4605 235.2002		
T= 235.2002	V= .4455		
T= 235.2002	V= .4455 236.0002		
T= 236.0002	V= .423		
T= 236.0002	V= .423 236.8002		
T= [illegible]	V= .3975 237.6002		
T= [illegible]	V= .3715 238.4002		
T= [illegible]	V= .3495 239.2002		
T= [illegible]	V= .3285 240.0002		
T= [illegible]	V= [illegible] 240.8002		
T= [illegible]	V= [illegible] 241.6002		
T= [illegible]	V= [illegible] 242.4002		
T= 242.4002	V= .2155 243.2002		
T= 243.2002	V= .1925		
T= 243.2002	V= .1925 244.0002		
T= 244.0002	V= .1765		
T= 244.0002	V= .1765 244.8002		
T= 244.8002	V= .163		
[illegible]	[illegible]		

Appendix 7: Program 'Readit'

```
LIST
01 REM PROGRAM "READIT"
02 REM TIME STEP 0.2 MS
03 REM   1. FIRST USE SMOOTH AND HZERO AS DESIRED
04 REM  2. THEN RETYPE LINE 05 TO REFLECT CURRENT WAVEFORM
05 RENAME TR2-H10,RACKET0
10 T=0
15 LPRINT "DISCRETE VOLTAGE vs TIME FOR RACKET IMPACT"
17 LPRINT
20 LPRINT "T= ";T;"     ";"V= ";RACKET0(T)
30 T=T+0.2
40 IF T>5 THEN GOTO 60
50 GOTO 20
60 END
█
```

Appendix 8: Voltage vs time listings for displacement history

```
DISCRETE VOLTAGE vs TIME FOR RACKET IMPACT
T=  0        V=  0
T=  0        V=  0 .2
T=  .2       V=  0
T=  .2       V=  0 .4
T=  .4       V=  0
T=  .4       V=  0 .6
T=  .6       V=   1.462397E-02
T=  .6       V=   1.462397E-02 .8
T=  .8       V=  .1023678
T=  .8       V=  .1023678 1
T=  1        V=  .3655992
T=  1        V=  .3655992 1.2
T=  1.2      V=  .8189423
T=  1.2      V=  .8189423 1.4
T=  1.4      V=  1.535517
T=  1.4      V=  1.535517 1.6
T=  1.6      V=  2.529947
T=  1.6      V=  2.529947 1.8
T=  1.8      V=  3.83148
T=  1.8      V=  3.83148 2
T=  2        V=  5.352373
T=  2        V=  5.352373 2.2
T=  2.2      V=  7.151121
T=  2.2      V=  7.151121 2.4
T=  2.4      V=  9.154605
T=  2.4      V=  9.154605 2.6
T=  2.6      V=  11.31895
T=  2.6      V=  11.31895 2.8
T=  2.8      V=  13.55642
T=  2.8      V=  13.55642 3
T=  3        V=  15.83776
T=  3        V=  15.83776 3.2
T=  3.2      V=  18.19222
T=  3.2      V=  18.19222 3.4
T=  3.4      V=  20.57593
T=  3.4      V=  20.57593 3.6
T=  3.6      V=  22.94501
T=  3.6      V=  22.94501 3.8
T=  3.8      V=  25.22635
T=  3.8      V=  25.22635 4
T=  4        V=  27.44919
T=  4        V=  27.44919 4.2

                          .4
```

Appendix 9: Transient analysis output - forces and moments

FEM TENNIS RACKET ANALYSIS - 1.0

TIME .0000E+00 SECONDS

BEAM ELEMENT INTERNAL FORCE RESULTS

NODE	U FORCE	V FORCE	W FORCE	U MOMENT	V MOMENT	W MOMENT
39	.0000E+00	.0000E+00	.0000E+00	.0000E+00	.0000E+00	.0000E+00

TIME 2.0000E-04 SECONDS

BEAM ELEMENT INTERNAL FORCE RESULTS

NODE	U FORCE	V FORCE	W FORCE	U MOMENT	V MOMENT	W MOMENT
39	.0000E+00	.0000E+00	.0000E+00	.0000E+00	.0000E+00	.0000E+00

TIME 4.0000E-04 SECONDS

BEAM ELEMENT INTERNAL FORCE RESULTS

NODE	U FORCE	V FORCE	W FORCE	U MOMENT	V MOMENT	W MOMENT
39	.0000E+00	.0000E+00	.0000E+00	.0000E+00	.0000E+00	.0000E+00

TIME 6.0000E-04 SECONDS

Appendix 9: (con't)

BEAM ELEMENT INTERNAL FORCE RESULTS

NODE	U FORCE	V FORCE	W FORCE	U MOMENT	V MOMENT	W MOMENT
39	-1.6433E-03	.0000E+00	1.9206E+00	.0000E+00	-1.6559E+00	.0000E+00

TIME 8.0000E-04 SECONDS

BEAM ELEMENT INTERNAL FORCE RESULTS

NODE	U FORCE	V FORCE	W FORCE	U MOMENT	V MOMENT	W MOMENT
39	-1.8071E-02	.0000E+00	1.2338E+01	.0000E+00	-9.8510E+00	.0000E+00

TIME 1.0000E-03 SECONDS

BEAM ELEMENT INTERNAL FORCE RESULTS

NODE	U FORCE	V FORCE	W FORCE	U MOMENT	V MOMENT	W MOMENT
39	-8.1563E-02	.0000E+00	4.3843E+01	.0000E+00	-3.1747E+01	.0000E+00

TIME 1.2000E-03 SECONDS

Appendix 9: (con't)

BEAM ELEMENT INTERNAL FORCE RESULTS

NODE	U FORCE	V FORCE	W FORCE	U MOMENT	V MOMENT	W MOMENT
39	-2.2037E-01	.0000E+00	9.9379E+01	.0000E+00	-6.3825E+01	.0000E+00

TIME 1.4000E-03 SECONDS

BEAM ELEMENT INTERNAL FORCE RESULTS

NODE	U FORCE	V FORCE	W FORCE	U MOMENT	V MOMENT	W MOMENT
39	-4.2030E-01	.0000E+00	1.9739E+02	.0000E+00	-1.2312E+02	.0000E+00

TIME 1.6000E-03 SECONDS

BEAM ELEMENT INTERNAL FORCE RESULTS

NODE	U FORCE	V FORCE	W FORCE	U MOMENT	V MOMENT	W MOMENT
39	-7.3291E-01	.0000E+00	3.1411E+02	.0000E+00	-1.9144E+02	.0000E+00

TIME 1.8000E-03 SECONDS

Appendix 9: (con't)

BEAM ELEMENT INTERNAL FORCE RESULTS

NODE	U FORCE	V FORCE	W FORCE	U MOMENT	V MOMENT	W MOMENT
39	-1.1445E+00	.0000E+00	4.8412E+02	.0000E+00	-2.8593E+02	.0000E+00

TIME 2.0000E-03 SECONDS

BEAM ELEMENT INTERNAL FORCE RESULTS

NODE	U FORCE	V FORCE	W FORCE	U MOMENT	V MOMENT	W MOMENT
39	-1.6888E+00	.0000E+00	6.7786E+02	.0000E+00	-3.9391E+02	.0000E+00

TIME 2.2000E-03 SECONDS

BEAM ELEMENT INTERNAL FORCE RESULTS

NODE	U FORCE	V FORCE	W FORCE	U MOMENT	V MOMENT	W MOMENT
39	-2.3537E+00	.0000E+00	9.2212E+02	.0000E+00	-5.0696E+02	.0000E+00

TIME 2.4000E-03 SECONDS

Appendix 9: (con't)

BEAM ELEMENT INTERNAL FORCE RESULTS

NODE	U FORCE	V FORCE	W FORCE	U MOMENT	V MOMENT	W MOMENT
39	-3.1318E+00	.0000E+00	1.1633E+03	.0000E+00	-6.1499E+02	.0000E+00

TIME 2.6000E-03 SECONDS

BEAM ELEMENT INTERNAL FORCE RESULTS

NODE	U FORCE	V FORCE	W FORCE	U MOMENT	V MOMENT	W MOMENT
39	-4.1000E+00	.0000E+00	1.4664E+03	.0000E+00	-7.4049E+02	.0000E+00

TIME 2.8000E-03 SECONDS

BEAM ELEMENT INTERNAL FORCE RESULTS

NODE	U FORCE	V FORCE	W FORCE	U MOMENT	V MOMENT	W MOMENT
39	-5.1174E+00	.0000E+00	1.7714E+03	.0000E+00	-8.5416E+02	.0000E+00

TIME 3.0000E-03 SECONDS

Appendix 9: (con't)

BEAM ELEMENT INTERNAL FORCE RESULTS

NODE	U FORCE	V FORCE	W FORCE	U MOMENT	V MOMENT	W MOMENT
39	-6.3526E+00	.0000E+00	2.0644E+03	.0000E+00	-9.3496E+02	.0000E+00

TIME 3.2000E-03 SECONDS

BEAM ELEMENT INTERNAL FORCE RESULTS

NODE	U FORCE	V FORCE	W FORCE	U MOMENT	V MOMENT	W MOMENT
39	-7.5058E+00	.0000E+00	2.4111E+03	.0000E+00	-1.0502E+03	.0000E+00

TIME 3.4000E-03 SECONDS

BEAM ELEMENT INTERNAL FORCE RESULTS

NODE	U FORCE	V FORCE	W FORCE	U MOMENT	V MOMENT	W MOMENT
39	-9.0256E+00	.0000E+00	2.7099E+03	.0000E+00	-1.1022E+03	.0000E+00

TIME 3.6000E-03 SECONDS

Appendix 9: (con't)

BEAM ELEMENT INTERNAL FORCE RESULTS

NODE	U FORCE	V FORCE	W FORCE	U MOMENT	V MOMENT	W MOMENT
39	-1.0445E+01	.0000E+00	3.0812E+03	.0000E+00	-1.1734E+03	.0000E+00

TIME 3.8000E-03 SECONDS

BEAM ELEMENT INTERNAL FORCE RESULTS

NODE	U FORCE	V FORCE	W FORCE	U MOMENT	V MOMENT	W MOMENT
39	-1.1880E+01	.0000E+00	3.3878E+03	.0000E+00	-1.2253E+03	.0000E+00

TIME 4.0000E-03 SECONDS

BEAM ELEMENT INTERNAL FORCE RESULTS

NODE	U FORCE	V FORCE	W FORCE	U MOMENT	V MOMENT	W MOMENT
39	-1.3552E+01	.0000E+00	3.6985E+03	.0000E+00	-1.2559E+03	.0000E+00

TIME 4.2000E-03 SECONDS

Appendix 10: Racket frame static deflection values

FEM TENNIS RACKET ANALYSIS - 1.0

STATIC DISPLACEMENT COMPONENTS

NODE	X TRANS	Y TRANS	Z TRANS	X ROT	Y ROT	Z ROT
1	.0000E+00	.0000E+00	5.0879E-02	.0000E+00	-3.9526E-03	.0000E+00
2	.0000E+00	.0000E+00	5.0681E-02	.0000E+00	-3.9513E-03	.0000E+00
3	.0000E+00	.0000E+00	5.0325E-02	.0000E+00	-3.9459E-03	.0000E+00
4	.0000E+00	.0000E+00	4.9813E-02	.0000E+00	-3.9373E-03	.0000E+00
5	.0000E+00	.0000E+00	4.8830E-02	.0000E+00	-3.9244E-03	.0000E+00
6	.0000E+00	.0000E+00	4.7497E-02	.0000E+00	-3.9125E-03	.0000E+00
7	.0000E+00	.0000E+00	4.5819E-02	.0000E+00	-3.8925E-03	.0000E+00
8	.0000E+00	.0000E+00	4.3956E-02	.0000E+00	-3.8685E-03	.0000E+00
9	.0000E+00	.0000E+00	4.1683E-02	.0000E+00	-3.8348E-03	.0000E+00
10	.0000E+00	.0000E+00	3.9849E-02	.0000E+00	-3.8062E-03	.0000E+00
11	.0000E+00	.0000E+00	3.8029E-02	.0000E+00	-3.7753E-03	.0000E+00
12	.0000E+00	.0000E+00	3.6187E-02	.0000E+00	-3.7427E-03	.0000E+00
13	.0000E+00	.0000E+00	3.4362E-02	.0000E+00	-3.7074E-03	.0000E+00
14	.0000E+00	.0000E+00	3.2775E-02	.0000E+00	-3.6743E-03	.0000E+00
15	.0000E+00	.0000E+00	3.0948E-02	.0000E+00	-3.6320E-03	.0000E+00
16	.0000E+00	.0000E+00	2.9394E-02	.0000E+00	-3.5929E-03	.0000E+00
17	.0000E+00	.0000E+00	2.7681E-02	.0000E+00	-3.5447E-03	.0000E+00
18	.0000E+00	.0000E+00	2.5958E-02	.0000E+00	-3.4893E-03	.0000E+00
19	.0000E+00	.0000E+00	2.4263E-02	.0000E+00	-3.4263E-03	.0000E+00
20	.0000E+00	.0000E+00	2.2635E-02	.0000E+00	-3.3590E-03	.0000E+00
21	.0000E+00	.0000E+00	2.1039E-02	.0000E+00	-3.2883E-03	.0000E+00
22	.0000E+00	.0000E+00	1.9419E-02	.0000E+00	-3.1888E-03	.0000E+00
23	.0000E+00	.0000E+00	1.7544E-02	.0000E+00	-3.0624E-03	.0000E+00
24	.0000E+00	.0000E+00	1.5893E-02	.0000E+00	-2.9399E-03	.0000E+00
25	.0000E+00	.0000E+00	1.4452E-02	.0000E+00	-2.8206E-03	.0000E+00
26	.0000E+00	.0000E+00	1.3344E-02	.0000E+00	-2.7225E-03	.0000E+00
27	.0000E+00	.0000E+00	1.2144E-02	.0000E+00	-2.6067E-03	.0000E+00
28	.0000E+00	.0000E+00	1.1374E-02	.0000E+00	-2.5267E-03	.0000E+00
29	.0000E+00	.0000E+00	1.0629E-02	.0000E+00	-2.4447E-03	.0000E+00
30	.0000E+00	.0000E+00	1.0026E-02	.0000E+00	-2.3725E-03	.0000E+00
31	.0000E+00	.0000E+00	9.4420E-03	.0000E+00	-2.3020E-03	.0000E+00
32	.0000E+00	.0000E+00	8.2199E-03	.0000E+00	-2.1407E-03	.0000E+00
33	.0000E+00	.0000E+00	7.1861E-03	.0000E+00	-1.9855E-03	.0000E+00
34	.0000E+00	.0000E+00	6.0458E-03	.0000E+00	-1.8209E-03	.0000E+00
35	.0000E+00	.0000E+00	4.9998E-03	.0000E+00	-1.6646E-03	.0000E+00
36	.0000E+00	.0000E+00	4.0472E-03	.0000E+00	-1.5097E-03	.0000E+00
37	.0000E+00	.0000E+00	3.1609E-03	.0000E+00	-1.3484E-03	.0000E+00
38	.0000E+00	.0000E+00	2.2245E-03	.0000E+00	-1.1471E-03	.0000E+00
39	.0000E+00	.0000E+00	8.2199E-04	.0000E+00	-7.1654E-04	.0000E+00
40	.0000E+00	.0000E+00	.0000E+00	.0000E+00	.0000E+00	.0000E+00

Appendix 11: Mode shape data

FEM TENNIS RACKET ANALYSIS - 1.0

MODE NO. 1 AT 3.03906E+01 CPS (1.90950E+02 RAD/SEC)

NODE	X TRANS	Y TRANS	Z TRANS	X ROT	Y ROT	Z ROT
1	-4.1561E-05	.0000E+00	-2.6749E-01	.0000E+00	1.8681E-02	.0000E+00
2	-4.1557E-05	.0000E+00	-2.6655E-01	.0000E+00	1.8684E-02	.0000E+00
3	-4.1619E-05	.0000E+00	-2.6487E-01	.0000E+00	1.8691E-02	.0000E+00
4	-4.1938E-05	.0000E+00	-2.6244E-01	.0000E+00	1.8701E-02	.0000E+00
5	-4.2133E-05	.0000E+00	-2.5777E-01	.0000E+00	1.8705E-02	.0000E+00
6	-4.2224E-05	.0000E+00	-2.5141E-01	.0000E+00	1.8706E-02	.0000E+00
7	-4.2355E-05	.0000E+00	-2.4336E-01	.0000E+00	1.9700E-02	.0000E+00
8	-4.2368E-05	.0000E+00	-2.3439E-01	.0000E+00	1.8689E-02	.0000E+00
9	-4.2423E-05	.0000E+00	-2.2337E-01	.0000E+00	1.8664E-02	.0000E+00
10	-4.2421E-05	.0000E+00	-2.1442E-01	.0000E+00	1.8636E-02	.0000E+00
11	-4.2360E-05	.0000E+00	-2.0548E-01	.0000E+00	1.8599E-02	.0000E+00
12	-4.2235E-05	.0000E+00	-1.9638E-01	.0000E+00	1.8553E-02	.0000E+00
13	-4.1830E-05	.0000E+00	-1.8730E-01	.0000E+00	1.8495E-02	.0000E+00
14	-4.1376E-05	.0000E+00	-1.7936E-01	.0000E+00	1.8432E-02	.0000E+00
15	-4.0698E-05	.0000E+00	-1.7017E-01	.0000E+00	1.8339E-02	.0000E+00
16	-4.0082E-05	.0000E+00	-1.6230E-01	.0000E+00	1.8240E-02	.0000E+00
17	-3.9509E-05	.0000E+00	-1.5358E-01	.0000E+00	1.8106E-02	.0000E+00
18	-3.8845E-05	.0000E+00	-1.4474E-01	.0000E+00	1.7941E-02	.0000E+00
19	-3.7935E-05	.0000E+00	-1.3600E-01	.0000E+00	1.7743E-02	.0000E+00
20	-3.6924E-05	.0000E+00	-1.2754E-01	.0000E+00	1.7519E-02	.0000E+00
21	-3.6104E-05	.0000E+00	-1.1919E-01	.0000E+00	1.7269E-02	.0000E+00
22	-3.5347E-05	.0000E+00	-1.1064E-01	.0000E+00	1.6897E-02	.0000E+00
23	-3.4379E-05	.0000E+00	-1.0065E-01	.0000E+00	1.6402E-02	.0000E+00
24	-3.3336E-05	.0000E+00	-9.1766E-02	.0000E+00	1.5899E-02	.0000E+00
25	-3.2290E-05	.0000E+00	-8.3941E-02	.0000E+00	1.5394E-02	.0000E+00
26	-3.1285E-05	.0000E+00	-7.7867E-02	.0000E+00	1.4969E-02	.0000E+00
27	-3.0125E-05	.0000E+00	-7.1245E-02	.0000E+00	1.4457E-02	.0000E+00
28	-2.9271E-05	.0000E+00	-6.6962E-02	.0000E+00	1.4097E-02	.0000E+00
29	-2.8202E-05	.0000E+00	-6.2788E-02	.0000E+00	1.3721E-02	.0000E+00
30	-2.7263E-05	.0000E+00	-5.9400E-02	.0000E+00	1.3384E-02	.0000E+00
31	-2.6282E-05	.0000E+00	-5.6095E-02	.0000E+00	1.3050E-02	.0000E+00
32	-2.4030E-05	.0000E+00	-4.9130E-02	.0000E+00	1.2268E-02	.0000E+00
33	-2.1777E-05	.0000E+00	-4.3187E-02	.0000E+00	1.1496E-02	.0000E+00
34	-1.9503E-05	.0000E+00	-3.6539E-02	.0000E+00	1.0654E-02	.0000E+00
35	-1.7410E-05	.0000E+00	-3.0389E-02	.0000E+00	9.8341E-03	.0000E+00
36	-1.5484E-05	.0000E+00	-2.4736E-02	.0000E+00	9.0006E-03	.0000E+00
37	-1.3610E-05	.0000E+00	-1.9429E-02	.0000E+00	8.1120E-03	.0000E+00
38	-1.1273E-05	.0000E+00	-1.3765E-02	.0000E+00	6.9764E-03	.0000E+00
39	-6.5871E-06	.0000E+00	-5.1527E-03	.0000E+00	4.4489E-03	.0000E+00
40	.0000E+00	.0000E+00	.0000E+00	.0000E+00	.0000E+00	.0000E+00

Appendix 11: (con't)

MODE NO. 2 AT 2.60846E+02 CPS (1.63894E+03 RAD/SEC)

NODE	X TRANS	Y TRANS	Z TRANS	X ROT	Y ROT	Z ROT
1	-1.5874E-05	.0000E+00	-2.0779E-01	.0000E+00	6.1922E-02	.0000E+00
2	-1.5869E-05	.0000E+00	-2.0470E-01	.0000E+00	6.1916E-02	.0000E+00
3	-1.5915E-05	.0000E+00	-1.9912E-01	.0000E+00	6.1868E-02	.0000E+00
4	-1.6160E-05	.0000E+00	-1.9109E-01	.0000E+00	6.1739E-02	.0000E+00
5	-1.6317E-05	.0000E+00	-1.7568E-01	.0000E+00	6.1457E-02	.0000E+00
6	-1.6390E-05	.0000E+00	-1.5483E-01	.0000E+00	6.1108E-02	.0000E+00
7	-1.6488E-05	.0000E+00	-1.2870E-01	.0000E+00	6.0380E-02	.0000E+00
8	-1.6514E-05	.0000E+00	-9.9943E-02	.0000E+00	5.9348E-02	.0000E+00
9	-1.6621E-05	.0000E+00	-6.5380E-02	.0000E+00	5.7701E-02	.0000E+00
10	-1.6715E-05	.0000E+00	-3.8033E-02	.0000E+00	5.6176E-02	.0000E+00
11	-1.6814E-05	.0000E+00	-1.1476E-02	.0000E+00	5.4414E-02	.0000E+00
12	-1.6925E-05	.0000E+00	1.4724E-02	.0000E+00	5.2465E-02	.0000E+00
13	-1.6880E-05	.0000E+00	3.9912E-02	.0000E+00	5.0289E-02	.0000E+00
14	-1.6769E-05	.0000E+00	6.1094E-02	.0000E+00	4.8195E-02	.0000E+00
15	-1.6602E-05	.0000E+00	8.4527E-02	.0000E+00	4.5485E-02	.0000E+00
16	-1.6491E-05	.0000E+00	1.0355E-01	.0000E+00	4.2958E-02	.0000E+00
17	-1.6470E-05	.0000E+00	1.2343E-01	.0000E+00	3.9858E-02	.0000E+00
18	-1.6400E-05	.0000E+00	1.4211E-01	.0000E+00	3.6317E-02	.0000E+00
19	-1.6182E-05	.0000E+00	1.5894E-01	.0000E+00	3.2361E-02	.0000E+00
20	-1.5945E-05	.0000E+00	1.7349E-01	.0000E+00	2.8222E-02	.0000E+00
21	-1.5840E-05	.0000E+00	1.8603E-01	.0000E+00	2.4011E-02	.0000E+00
22	-1.5771E-05	.0000E+00	1.9661E-01	.0000E+00	1.8299E-02	.0000E+00
23	-1.5634E-05	.0000E+00	2.0553E-01	.0000E+00	1.1426E-02	.0000E+00
24	-1.5526E-05	.0000E+00	2.1010E-01	.0000E+00	5.2041E-03	.0000E+00
25	-1.5459E-05	.0000E+00	2.1129E-01	.0000E+00	-4.1765E-04	.0000E+00
26	-1.5173E-05	.0000E+00	2.1026E-01	.0000E+00	-4.7085E-03	.0000E+00
27	-1.4812E-05	.0000E+00	2.0708E-01	.0000E+00	-9.3882E-03	.0000E+00
28	-1.4500E-05	.0000E+00	2.0381E-01	.0000E+00	-1.2369E-02	.0000E+00
29	-1.4034E-05	.0000E+00	1.9967E-01	.0000E+00	-1.5217E-02	.0000E+00
30	-1.3637E-05	.0000E+00	1.9557E-01	.0000E+00	-1.7546E-02	.0000E+00
31	-1.3180E-05	.0000E+00	1.9092E-01	.0000E+00	-1.9654E-02	.0000E+00
32	-1.2201E-05	.0000E+00	1.7892E-01	.0000E+00	-2.3878E-02	.0000E+00
33	-1.1186E-05	.0000E+00	1.6613E-01	.0000E+00	-2.7159E-02	.0000E+00
34	-1.0100E-05	.0000E+00	1.4901E-01	.0000E+00	-2.9761E-02	.0000E+00
35	-9.1811E-06	.0000E+00	1.3064E-01	.0000E+00	-3.1322E-02	.0000E+00
36	-8.2981E-06	.0000E+00	1.1161E-01	.0000E+00	-3.1977E-02	.0000E+00
37	-7.3167E-06	.0000E+00	9.1810E-02	.0000E+00	-3.1735E-02	.0000E+00
38	-6.1293E-06	.0000E+00	6.8505E-02	.0000E+00	-3.0177E-02	.0000E+00
39	-3.8703E-06	.0000E+00	2.8116E-02	.0000E+00	-2.2679E-02	.0000E+00
40	.0000E+00	.0000E+00	.0000E+00	.0000E+00	.0000E+00	.0000E+00

Appendix 11: (con't)

MODE NO. 3 AT 7.72698E+02 CPS (4.85500E+03 RAD/SEC)

NODE	X TRANS	Y TRANS	Z TRANS	X ROT	Y ROT	Z ROT
1	2.3182E-05	.0000E+00	-1.9586E-01	.0000E+00	1.1510E-01	.0000E+00
2	2.3172E-05	.0000E+00	-1.9010E-01	.0000E+00	1.1503E-01	.0000E+00
3	2.3071E-05	.0000E+00	-1.7976E-01	.0000E+00	1.1456E-01	.0000E+00
4	2.2779E-05	.0000E+00	-1.6492E-01	.0000E+00	1.1342E-01	.0000E+00
5	2.2571E-05	.0000E+00	-1.3680E-01	.0000E+00	1.1102E-01	.0000E+00
6	2.2471E-05	.0000E+00	-9.9472E-02	.0000E+00	1.0817E-01	.0000E+00
7	2.2326E-05	.0000E+00	-5.4079E-02	.0000E+00	1.0239E-01	.0000E+00
8	2.2210E-05	.0000E+00	-5.6825E-03	.0000E+00	9.4518E-02	.0000E+00
9	2.1943E-05	.0000E+00	4.5768E-02	.0000E+00	8.2559E-02	.0000E+00
10	2.1691E-05	.0000E+00	8.2963E-02	.0000E+00	7.2058E-02	.0000E+00
11	2.1399E-05	.0000E+00	1.1487E-01	.0000E+00	6.0583E-02	.0000E+00
12	2.1067E-05	.0000E+00	1.4169E-01	.0000E+00	4.8654E-02	.0000E+00
13	2.0826E-05	.0000E+00	1.6251E-01	.0000E+00	3.6202E-02	.0000E+00
14	2.0602E-05	.0000E+00	1.7570E-01	.0000E+00	2.5033E-02	.0000E+00
15	2.0257E-05	.0000E+00	1.8488E-01	.0000E+00	1.1660E-02	.0000E+00
16	1.9832E-05	.0000E+00	1.8744E-01	.0000E+00	2.1997E-04	.0000E+00
17	1.9159E-05	.0000E+00	1.8446E-01	.0000E+00	-1.2534E-02	.0000E+00
18	1.8400E-05	.0000E+00	1.7511E-01	.0000E+00	-2.5501E-02	.0000E+00
19	1.7632E-05	.0000E+00	1.5947E-01	.0000E+00	-3.8120E-02	.0000E+00
20	1.6818E-05	.0000E+00	1.3842E-01	.0000E+00	-4.9323E-02	.0000E+00
21	1.5980E-05	.0000E+00	1.1244E-01	.0000E+00	-5.8643E-02	.0000E+00
22	1.4885E-05	.0000E+00	8.0570E-02	.0000E+00	-6.8321E-02	.0000E+00
23	1.3660E-05	.0000E+00	3.7093E-02	.0000E+00	-7.5817E-02	.0000E+00
24	1.2490E-05	.0000E+00	-5.5416E-03	.0000E+00	-7.8536E-02	.0000E+00
25	1.1175E-05	.0000E+00	-4.4698E-02	.0000E+00	-7.7519E-02	.0000E+00
26	1.0323E-05	.0000E+00	-7.5150E-02	.0000E+00	-7.4395E-02	.0000E+00
27	9.5246E-06	.0000E+00	-1.0739E-01	.0000E+00	-6.8487E-02	.0000E+00
28	9.0539E-06	.0000E+00	-1.2718E-01	.0000E+00	-6.3265E-02	.0000E+00
29	8.5419E-06	.0000E+00	-1.4526E-01	.0000E+00	-5.7110E-02	.0000E+00
30	8.0468E-06	.0000E+00	-1.5880E-01	.0000E+00	-5.1162E-02	.0000E+00
31	7.6861E-06	.0000E+00	-1.7083E-01	.0000E+00	-4.4977E-02	.0000E+00
32	6.9057E-06	.0000E+00	-1.9148E-01	.0000E+00	-2.9820E-02	.0000E+00
33	6.1563E-06	.0000E+00	-2.0263E-01	.0000E+00	-1.4666E-02	.0000E+00
34	5.5163E-06	.0000E+00	-2.0668E-01	.0000E+00	1.1882E-03	.0000E+00
35	4.7973E-06	.0000E+00	-2.0172E-01	.0000E+00	1.5195E-02	.0000E+00
36	4.1725E-06	.0000E+00	-1.8988E-01	.0000E+00	2.7338E-02	.0000E+00
37	3.7021E-06	.0000E+00	-1.6866E-01	.0000E+00	3.7496E-02	.0000E+00
38	3.0946E-06	.0000E+00	-1.3708E-01	.0000E+00	4.5967E-02	.0000E+00
39	1.9134E-06	.0000E+00	-6.4420E-02	.0000E+00	4.7003E-02	.0000E+00
40	.0000E+00	.0000E+00	.0000E+00	.0000E+00	.0000E+00	.0000E+00

Appendix 11: (con't)

MODE NO. 4 AT 1.48295E+03 CPS (9.31763E+03 RAD/SEC)

NODE	X TRANS	Y TRANS	Z TRANS	X ROT	Y ROT	Z ROT
1	-5.5404E-05	.0000E+00	1.8432E-01	.0000E+00	-1.7466E-01	.0000E+00
2	-5.5282E-05	.0000E+00	1.7558E-01	.0000E+00	-1.7434E-01	.0000E+00
3	-5.4792E-05	.0000E+00	1.5993E-01	.0000E+00	-1.7245E-01	.0000E+00
4	-5.4103E-05	.0000E+00	1.3771E-01	.0000E+00	-1.6821E-01	.0000E+00
5	-5.3498E-05	.0000E+00	9.6506E-02	.0000E+00	-1.5977E-01	.0000E+00
6	-5.3154E-05	.0000E+00	4.3617E-02	.0000E+00	-1.5018E-01	.0000E+00
7	-5.2674E-05	.0000E+00	-1.7337E-02	.0000E+00	-1.3164E-01	.0000E+00
8	-5.2190E-05	.0000E+00	-7.5137E-02	.0000E+00	-1.0771E-01	.0000E+00
9	-5.1431E-05	.0000E+00	-1.2916E-01	.0000E+00	-7.3876E-02	.0000E+00
10	-5.0771E-05	.0000E+00	-1.5619E-01	.0000E+00	-4.5502E-02	.0000E+00
11	-5.0072E-05	.0000E+00	-1.7399E-01	.0000E+00	-1.9075E-02	.0000E+00
12	-4.9346E-05	.0000E+00	-1.7703E-01	.0000E+00	6.6397E-03	.0000E+00
13	-4.8690E-05	.0000E+00	-1.6792E-01	.0000E+00	3.0325E-02	.0000E+00
14	-4.8083E-05	.0000E+00	-1.5085E-01	.0000E+00	4.8730E-02	.0000E+00
15	-4.7275E-05	.0000E+00	-1.2175E-01	.0000E+00	6.7046E-02	.0000E+00
16	-4.6482E-05	.0000E+00	-9.0167E-02	.0000E+00	7.9279E-02	.0000E+00
17	-4.5436E-05	.0000E+00	-4.9633E-02	.0000E+00	8.8798E-02	.0000E+00
18	-4.4283E-05	.0000E+00	-4.7391E-03	.0000E+00	9.3498E-02	.0000E+00
19	-4.3015E-05	.0000E+00	4.1063E-02	.0000E+00	9.2443E-02	.0000E+00
20	-4.1611E-05	.0000E+00	8.4013E-02	.0000E+00	8.5586E-02	.0000E+00
21	-4.0183E-05	.0000E+00	1.2243E-01	.0000E+00	7.3694E-02	.0000E+00
22	-3.8323E-05	.0000E+00	1.5410E-01	.0000E+00	5.2105E-02	.0000E+00
23	-3.6075E-05	.0000E+00	1.7626E-01	.0000E+00	2.1040E-02	.0000E+00
24	-3.3883E-05	.0000E+00	1.7947E-01	.0000E+00	-9.4825E-03	.0000E+00
25	-3.1627E-05	.0000E+00	1.6778E-01	.0000E+00	-3.6963E-02	.0000E+00
26	-2.9905E-05	.0000E+00	1.4898E-01	.0000E+00	-5.6626E-02	.0000E+00
27	-2.7969E-05	.0000E+00	1.1908E-01	.0000E+00	-7.5513E-02	.0000E+00
28	-2.6715E-05	.0000E+00	9.4872E-02	.0000E+00	-8.5498E-02	.0000E+00
29	-2.5390E-05	.0000E+00	6.8023E-02	.0000E+00	-9.3056E-02	.0000E+00
30	-2.4251E-05	.0000E+00	4.4165E-02	.0000E+00	-9.7475E-02	.0000E+00
31	-2.3296E-05	.0000E+00	1.9464E-02	.0000E+00	-9.9798E-02	.0000E+00
32	-2.1166E-05	.0000E+00	-3.5385E-02	.0000E+00	-9.8026E-02	.0000E+00
33	-1.9078E-05	.0000E+00	-8.2255E-02	.0000E+00	-8.8167E-02	.0000E+00
34	-1.7067E-05	.0000E+00	-1.3019E-01	.0000E+00	-7.0261E-02	.0000E+00
35	-1.5204E-05	.0000E+00	-1.6588E-01	.0000E+00	-4.7852E-02	.0000E+00
36	-1.3517E-05	.0000E+00	-1.8720E-01	.0000E+00	-2.2795E-02	.0000E+00
37	-1.1867E-05	.0000E+00	-1.9319E-01	.0000E+00	3.4420E-03	.0000E+00
38	-9.8875E-06	.0000E+00	-1.7945E-01	.0000E+00	3.2373E-02	.0000E+00
39	-6.0998E-06	.0000E+00	-1.0121E-01	.0000E+00	6.4304E-02	.0000E+00
40	.0000E+00	.0000E+00	.0000E+00	.0000E+00	.0000E+00	.0000E+00

Appendix 11: (con't)

MODE NO. 5 AT 2.07301E+03 CPS (1.30251E+04 RAD/SEC)

NODE	X TRANS	Y TRANS	Z TRANS	X ROT	Y ROT	Z ROT
1	-2.2242E-01	.0000E+00	5.6562E-05	.0000E+00	-3.2504E-05	.0000E+00
2	-2.2144E-01	.0000E+00	5.4854E-05	.0000E+00	-3.6433E-05	.0000E+00
3	-2.1802E-01	.0000E+00	5.1280E-05	.0000E+00	-4.0424E-05	.0000E+00
4	-2.1445E-01	.0000E+00	4.6206E-05	.0000E+00	-3.6723E-05	.0000E+00
5	-2.1103E-01	.0000E+00	3.7614E-05	.0000E+00	-3.2132E-05	.0000E+00
6	-2.0896E-01	.0000E+00	2.7621E-05	.0000E+00	-2.5899E-05	.0000E+00
7	-2.0615E-01	.0000E+00	1.8746E-05	.0000E+00	-1.4322E-05	.0000E+00
8	-2.0332E-01	.0000E+00	1.5359E-05	.0000E+00	1.4262E-06	.0000E+00
9	-1.9985E-01	.0000E+00	2.2441E-05	.0000E+00	2.2794E-05	.0000E+00
10	-1.9721E-01	.0000E+00	3.6633E-05	.0000E+00	3.5808E-05	.0000E+00
11	-1.9455E-01	.0000E+00	5.5593E-05	.0000E+00	4.1789E-05	.0000E+00
12	-1.9190E-01	.0000E+00	7.6260E-05	.0000E+00	4.1495E-05	.0000E+00
13	-1.8919E-01	.0000E+00	9.5634E-05	.0000E+00	3.6992E-05	.0000E+00
14	-1.8674E-01	.0000E+00	1.1026E-04	.0000E+00	3.0703E-05	.0000E+00
15	-1.8372E-01	.0000E+00	1.2302E-04	.0000E+00	1.9185E-05	.0000E+00
16	-1.8101E-01	.0000E+00	1.2847E-04	.0000E+00	5.6487E-06	.0000E+00
17	-1.7776E-01	.0000E+00	1.2699E-04	.0000E+00	-1.1702E-05	.0000E+00
18	-1.7411E-01	.0000E+00	1.1707E-04	.0000E+00	-2.8573E-05	.0000E+00
19	-1.7005E-01	.0000E+00	9.8987E-05	.0000E+00	-4.4863E-05	.0000E+00
20	-1.6578E-01	.0000E+00	7.4123E-05	.0000E+00	-5.8073E-05	.0000E+00
21	-1.6139E-01	.0000E+00	4.3877E-05	.0000E+00	-6.7060E-05	.0000E+00
22	-1.5522E-01	.0000E+00	8.7799E-06	.0000E+00	-7.2077E-05	.0000E+00
23	-1.4751E-01	.0000E+00	-3.3877E-05	.0000E+00	-6.8449E-05	.0000E+00
24	-1.4018E-01	.0000E+00	-6.8624E-05	.0000E+00	-5.6825E-05	.0000E+00
25	-1.3316E-01	.0000E+00	-9.3236E-05	.0000E+00	-4.0947E-05	.0000E+00
26	-1.2751E-01	.0000E+00	-1.0678E-04	.0000E+00	-2.6410E-05	.0000E+00
27	-1.2090E-01	.0000E+00	-1.1480E-04	.0000E+00	-9.1713E-06	.0000E+00
28	-1.1644E-01	.0000E+00	-1.1582E-04	.0000E+00	2.3139E-06	.0000E+00
29	-1.1190E-01	.0000E+00	-1.1352E-04	.0000E+00	1.3173E-05	.0000E+00
30	-1.0797E-01	.0000E+00	-1.0910E-04	.0000E+00	2.2152E-05	.0000E+00
31	-1.0418E-01	.0000E+00	-1.0251E-04	.0000E+00	3.0373E-05	.0000E+00
32	-9.5475E-02	.0000E+00	-8.1405E-05	.0000E+00	4.5703E-05	.0000E+00
33	-8.7266E-02	.0000E+00	-5.5842E-05	.0000E+00	5.5587E-05	.0000E+00
34	-7.8833E-02	.0000E+00	-2.1126E-05	.0000E+00	5.8752E-05	.0000E+00
35	-7.1076E-02	.0000E+00	1.3276E-05	.0000E+00	5.4782E-05	.0000E+00
36	-6.3603E-02	.0000E+00	4.3338E-05	.0000E+00	4.4419E-05	.0000E+00
37	-5.6044E-02	.0000E+00	6.6239E-05	.0000E+00	2.8706E-05	.0000E+00
38	-4.5904E-02	.0000E+00	7.9558E-05	.0000E+00	6.4471E-06	.0000E+00
39	-2.8320E-02	.0000E+00	5.8578E-05	.0000E+00	-3.0200E-05	.0000E+00
40	.0000E+00	.0000E+00	.0000E+00	.0000E+00	.0000E+00	.0000E+00

Appendix 11: (con't)

MODE NO. 6 AT 2.40500E+03 CPS (1.51111E+04 RAD/SEC)

NODE	X TRANS	Y TRANS	Z TRANS	X ROT	Y ROT	Z ROT
1	-4.8656E-05	.0000E+00	-1.5711E-01	.0000E+00	2.1921E-01	.0000E+00
2	-4.8364E-05	.0000E+00	-1.4615E-01	.0000E+00	2.1825E-01	.0000E+00
3	-4.7387E-05	.0000E+00	-1.2663E-01	.0000E+00	2.1326E-01	.0000E+00
4	-4.6536E-05	.0000E+00	-9.9408E-02	.0000E+00	2.0296E-01	.0000E+00
5	-4.5677E-05	.0000E+00	-5.0637E-02	.0000E+00	1.8378E-01	.0000E+00
6	-4.5144E-05	.0000E+00	8.7324E-03	.0000E+00	1.6317E-01	.0000E+00
7	-4.4437E-05	.0000E+00	7.1459E-02	.0000E+00	1.2563E-01	.0000E+00
8	-4.3755E-05	.0000E+00	1.2146E-01	.0000E+00	8.0567E-02	.0000E+00
9	-4.3105E-05	.0000E+00	1.5244E-01	.0000E+00	2.3137E-02	.0000E+00
10	-4.2683E-05	.0000E+00	1.5374E-01	.0000E+00	-1.7642E-02	.0000E+00
11	-4.2268E-05	.0000E+00	1.3670E-01	.0000E+00	-5.2609E-02	.0000E+00
12	-4.1840E-05	.0000E+00	1.0417E-01	.0000E+00	-7.8950E-02	.0000E+00
13	-4.1281E-05	.0000E+00	6.0922E-02	.0000E+00	-9.6097E-02	.0000E+00
14	-4.0768E-05	.0000E+00	1.7842E-02	.0000E+00	-1.0303E-01	.0000E+00
15	-4.0160E-05	.0000E+00	-3.3719E-02	.0000E+00	-1.0149E-01	.0000E+00
16	-3.9621E-05	.0000E+00	-7.5619E-02	.0000E+00	-9.2209E-02	.0000E+00
17	-3.8953E-05	.0000E+00	-1.1575E-01	.0000E+00	-7.3757E-02	.0000E+00
18	-3.8089E-05	.0000E+00	-1.4558E-01	.0000E+00	-4.6999E-02	.0000E+00
19	-3.7132E-05	.0000E+00	-1.6067E-01	.0000E+00	-1.4076E-02	.0000E+00
20	-3.6234E-05	.0000E+00	-1.5919E-01	.0000E+00	2.0148E-02	.0000E+00
21	-3.5331E-05	.0000E+00	-1.4179E-01	.0000E+00	5.1668E-02	.0000E+00
22	-3.3982E-05	.0000E+00	-1.0693E-01	.0000E+00	8.6116E-02	.0000E+00
23	-3.2341E-05	.0000E+00	-4.6592E-02	.0000E+00	1.1172E-01	.0000E+00
24	-3.0831E-05	.0000E+00	1.7128E-02	.0000E+00	1.1688E-01	.0000E+00
25	-2.9397E-05	.0000E+00	7.3397E-02	.0000E+00	1.0568E-01	.0000E+00
26	-2.8257E-05	.0000E+00	1.1221E-01	.0000E+00	8.7052E-02	.0000E+00
27	-2.7053E-05	.0000E+00	1.4501E-01	.0000E+00	5.7425E-02	.0000E+00
28	-2.6228E-05	.0000E+00	1.5880E-01	.0000E+00	3.4131E-02	.0000E+00
29	-2.5423E-05	.0000E+00	1.6533E-01	.0000E+00	9.2410E-03	.0000E+00
30	-2.4707E-05	.0000E+00	1.6491E-01	.0000E+00	-1.2553E-02	.0000E+00
31	-2.3943E-05	.0000E+00	1.5920E-01	.0000E+00	-3.2994E-02	.0000E+00
32	-2.2166E-05	.0000E+00	1.2945E-01	.0000E+00	-7.3741E-02	.0000E+00
33	-2.0514E-05	.0000E+00	8.5155E-02	.0000E+00	-1.0144E-01	.0000E+00
34	-1.8829E-05	.0000E+00	1.9387E-02	.0000E+00	-1.1479E-01	.0000E+00
35	-1.7171E-05	.0000E+00	-4.8964E-02	.0000E+00	-1.1021E-01	.0000E+00
36	-1.5381E-05	.0000E+00	-1.0990E-01	.0000E+00	-9.0522E-02	.0000E+00
37	-1.3627E-05	.0000E+00	-1.5658E-01	.0000E+00	-5.8345E-02	.0000E+00
38	-1.1506E-05	.0000E+00	-1.8279E-01	.0000E+00	-1.0716E-02	.0000E+00
39	-6.9013E-06	.0000E+00	-1.3247E-01	.0000E+00	6.8848E-02	.0000E+00
40	.0000E+00	.0000E+00	.0000E+00	.0000E+00	.0000E+00	.0000E+00

MODE 2 EIGENVECTOR ERROR PRODUCT 2.713E-03
LARGEST EIGENVECTOR ERROR PRODUCT 2.713E-03 AT MODE 2

==

Appendix 12: Transient analysis output - displacement

FEM TENNIS RACKET ANALYSIS - 1.0

DISPLACEMENT LISTING

TIME	ZT 1	ZT 15
+0.0000E+00	+0.0000E+00	+0.0000E+00
+2.0000E-04	+0.0000E+00	+0.0000E+00
+4.0000E-04	+0.0000E+00	+0.0000E+00
+6.0000E-04	+5.6356E-04	-1.3341E-04
+8.0000E-04	+3.9372E-03	-8.4174E-04
+1.0000E-03	+1.4128E-02	-2.6944E-03
+1.2000E-03	+3.1613E-02	-5.1554E-03
+1.4000E-03	+5.9444E-02	-8.8132E-03
+1.6000E-03	+9.7658E-02	-1.2916E-02
+1.8000E-03	+1.4784E-01	-1.6400E-02
+2.0000E-03	+2.0651E-01	-1.8118E-02
+2.2000E-03	+2.7599E-01	-1.7126E-02
+2.4000E-03	+3.5319E-01	-1.2318E-02
+2.6000E-03	+4.3618E-01	-1.2239E-03
+2.8000E-03	+5.2496E-01	+1.5126E-02
+3.0000E-03	+6.0988E-01	+4.0860E-02
+3.2000E-03	+7.0252E-01	+7.0754E-02
+3.4000E-03	+7.9516E-01	+1.0845E-01
+3.6000E-03	+8.8394E-01	+1.5481E-01
+3.8000E-03	+9.7272E-01	+2.0093E-01
+4.0000E-03	+1.0576E+00	+2.5463E-01